



# Analytical investigation for true and spurious eigensolutions of multiply-connected membranes containing elliptical boundaries using the dual BIEM

Jeng Tzong Chen<sup>a,b,\*</sup>, Jia Wei Lee<sup>a</sup>, Shyue Yuh Leu<sup>c</sup>

<sup>a</sup> Department of Harbor and River Engineering, National Taiwan Ocean University, Keelung, Taiwan

<sup>b</sup> Department of Mechanical and Mechatronic Engineering, National Taiwan Ocean University, Keelung, Taiwan

<sup>c</sup> Department of Aviation Mechanical Engineering, China University of Science and Technology, Hsinchu, Taiwan

## ARTICLE INFO

### Article history:

Received 27 April 2010

Received in revised form 10 October 2010

Available online 13 November 2010

### Keywords:

Spurious eigenvalues

Elliptic coordinates

Mathieu functions

Jacobian term

Separable kernel

## ABSTRACT

It is well known that the boundary element method may induce spurious eigenvalues while solving eigenvalue problems. The finding that spurious eigenvalues depend on the geometry of inner boundary and the approach utilized has been revealed analytically and numerically in the literature. However, all the related efforts were focused on eigenproblems involving circular boundaries. On the other hand, the extension to elliptical boundaries seems not straightforward and lacks of attention. Accordingly, this paper performs an analytical investigation of spurious eigenvalues for a confocal elliptical membrane using boundary integral equation methods (BIEM) in conjunction with separable kernels and eigenfunction expansion. To analytically study this eigenproblem, the elliptic coordinates and Mathieu functions are adopted. The fundamental solution is expanded into the separable kernel by using the elliptic coordinates and the boundary densities are expanded by using the eigenfunction expansion. The Jacobian terms may exist in the separable kernel, boundary density and boundary contour integration and they can cancel each other out. Therefore, the orthogonal relations are reserved in the boundary contour integration. In this way, a similar finding about the mechanism of spurious eigenvalues is found and agrees with those corresponding to the annular case. To verify this finding, the boundary element method and the commercial finite-element code ABAQUS are also utilized to provide eigensolutions, respectively, for comparisons. Good agreement is observed from comparisons. Based on the adaptive observer system, the present approach can deal with eigenproblems containing circular and elliptical boundaries at the same time in a semi-analytical manner. By using the BIEM, it is found that spurious eigenvalues are the zeros of the modified Mathieu functions which depend on the inner elliptical boundary and the integral formulation. Finally, several methods including the CHIEF method, the SVD updating technique and the Burton & Miller method are employed to filter out the spurious eigenvalues, respectively. In addition, the efficiency of the CHIEF method is better than those of the SVD updating technique and the Burton & Miller approach, since not only hypersingularity is avoided but also computation effort is saved.

© 2010 Elsevier Ltd. All rights reserved.

## 1. Introduction

Eigenanalysis is very important for vibration and acoustics, because it can provide some fundamental information. Since analytical solutions are sometimes not available, numerical methods are needed. In recent years, several numerical methods were utilized to determine eigenvalues and eigenmodes such as the finite element method (FEM) or the boundary element method (BEM). Although the FEM is a popular method, it needs to generate the

mesh over the whole domain. The BEM only generates the mesh on the boundary but it may face with the calculation of the principal value and the pollution of spurious eigenvalues. Tai and Shaw (1974) first employed the complex-valued BEM to solve membrane vibration. De Mey (1976) revisited this problem in 1976. Later, De Mey (1977) proposed a simplified approach by using only the real-part or imaginary-part kernel where he found that spurious solutions were imbedded as well as the ill-posed matrix appeared. In a similar way of using the real-part kernel, Hutchinson and Wong (1979) and Hutchinson (1984) solved the free vibration of plate. Also, Yasko (2000) as well as Duran et al. (2001) employed the real-part kernel approach. It is interesting to find that Kang et al. (1999) proposed a non-dimensional influence function (NDIF) method which was an imaginary-part kernel approach as

\* Corresponding author at: Department of Harbor and River Engineering, National Taiwan Ocean University, Keelung, Taiwan. Tel.: +886 2 24622192x6177; fax: +886 2 24632375.

E-mail address: [jtchen@mail.ntou.edu.tw](mailto:jtchen@mail.ntou.edu.tw) (J.T. Chen).

commented by [Chen et al. \(2002\)](#), [Kamiya et al. \(1996\)](#) and [Yeih et al. \(1998\)](#) linked the relation of the multiple reciprocity method (MRM) and real-part BEM independently. This is the reason why spurious eigenvalues are also inherent in these two methods, the MRM and the real-part BEM. However, no proof was given at that time. Until 2000, [Kuo et al. \(2000\)](#) proved the existence of spurious eigensolutions and pointed out that spurious eigenvalues occur at the zeros of the  $m$ th-order Bessel functions of the second kind or their derivatives through a circular membrane for the real-part dual BEM. Later, [Chen et al. \(2004a\)](#), [Lee and Chen \(2008a\)](#) extended a circular membrane to a circular plate by using the real-part BEM and BIEM, respectively.

Appearance of spurious eigensolutions for simply-connected problems was due to the loss of constraint by only using the real or the imaginary-part kernel ([Kuo et al., 2000](#); [Chen et al., 2009a](#)). [Tai and Shaw \(1974\)](#) claimed that spurious eigenvalues do not appear if the complex-valued kernels are employed. However, it is true only for simply-connected domain. Even though we employ the complex-valued kernels for the multiply-connected eigenproblems, the spurious eigensolutions also occur ([Kitahara, 1985](#); [Chen et al., 2001, 2003](#)). [Kobayashi and Nishimura \(1982\)](#) have identified that spurious eigenvalues (irregular frequencies) for multiply-connected domains using the singular formulation are the eigenfrequencies of the Dirichlet problem containing the inner boundary. From their arguments, it is quite obvious that the spurious eigenvalues in the singular (resp. hypersingular) formulation for multiply-connected domains are the Dirichlet (resp. Neumann) eigenfrequencies of problems containing the inner boundary. Since the doubly-connected eigenproblem can be decomposed into two parts, one is an exterior problem bounded by interior boundary and the other is an interior problem. Mathematically speaking, a spurious eigenvalue for the doubly-connected problem originates from the same fictitious frequency for the exterior part problem. It is interesting to find that the spurious eigenvalues of the annular domain depend on the geometry of inner boundary and the integral formulation. This finding was analytically verified by [Chen et al. \(2003\)](#). This finding is the same with the viewpoint of [Kobayashi and Nishimura \(1982\)](#).

It is well known that fictitious frequency appears in the exterior Helmholtz problem. The Burton & Miller approach ([Burton and Miller, 1971](#)) and the combined Helmholtz interior integral equation formulation (CHIEF) method ([Schenck, 1968](#); [Seybert and Rengarajan, 1987](#)) have been proposed to deal with the fictitious frequency problem of the exterior acoustics. Furthermore, [Chen et al. \(2001, 2003, 2007\)](#) extended the Burton & Miller approach as well as the CHIEF method to filter out the spurious eigenvalues for the multiply-connected eigenproblems. Spurious eigenvalues can be fully filtered out by using the Burton & Miller approach, but it needs the computation of the hypersingular equation. The CHIEF method may fail if one uses inappropriate CHIEF points in order to add independent equations. If the location of the CHIEF point is located on the nodal line of the interior problems ([Chen et al., 2003](#)), the appearance of fictitious frequency may not be suppressed. Besides, [Chen and his co-workers \(2003, 2004b, 2005, 2007, 2008b, 2009a, 2010a\)](#) employed the singular value decomposition (SVD) updating technique to detect spurious eigenvalues. Not only true eigenvalues but also spurious eigenvalues can be extracted out by using the SVD updating terms and SVD updating documents, respectively. This technique has been successfully employed for rod ([Chen et al., 2009a](#)), circular membrane ([Chen et al., 2003, 2005, 2007](#)), plate ([Lee and Chen, 2008b](#)) and concentric sphere cavity ([Chen et al., 2010a](#)).

[Chen et al. \(2001, 2003\)](#) studied spurious eigenvalues of circular membranes in both the continuous and discrete systems by using the separable kernel and circulant, respectively. Note that the term

of the separable kernel is adopted in the paper to imply an infinite-rank expansion of a closed-form fundamental solution. It is to avoid the confusion with the degenerate kernel defined by [Courant and Hilbert \(1989\)](#) to be a kernel with a finite-rank expansion to approximate the closed-form fundamental solution. In numerical implementation, we adopt the separate kernel for the fundamental solution since finite terms of expansion are considered. In the paper, we aim to extend successful experiences in annular membranes ([Chen et al., 2001, 2003](#)) to deal with eigenproblems containing elliptical boundaries. However, the circulant property is no longer present for the ellipse. A special care should be taken to derive a separable kernel in the elliptic coordinates which is not straightforward to obtain. Regarding eigenproblems with elliptical boundaries, [Troesch and Troesch \(1973\)](#) used the separation of variables to obtain the eigenfrequencies and nodal patterns of an elliptic membrane. [Hong and Kim \(1995\)](#) also employed the separation of variables to determine the natural mode of hollow and elliptical annulus for cylindrical cavities. Both the elliptic coordinates and the Mathieu functions were used in the previous investigations.

Recently, [Chen et al. \(2007\)](#) developed the null-field boundary integral equation method (BIEM) in conjunction with the separable kernel and the Fourier series to solve the eigenproblems containing circular boundaries. By introducing the separable kernels, the calculation of the singular and hypersingular integrations in the sense of principal value by using bump contour are free when the collocation point is exactly located on the real boundary. This approach is one kind of semi-analytical and meshless methods. Later, [Chen et al. \(2010b\)](#) extend the BIEM to deal with torsion problems containing multiple elliptical inclusions. The key point is that the separable kernel in terms of the elliptic coordinates is available in the [Morse and Feshbach's book \(1953\)](#).

In this paper, we will derive the BIE formulations and extend to solve eigenproblems containing elliptical boundaries. The BIEM is utilized in conjunction with the separable kernel and the eigenfunction expansion for the closed-form fundamental solution and boundary densities, respectively. To fully utilize the elliptical geometry, the elliptic coordinates in companion with the Mathieu function ([Morse and Feshbach, 1953](#); [Abramowitz and Stegun, 1965](#); [Zhang and Jin, 1996](#)) are used. The fundamental solution is expanded to the separable kernel by using the elliptic coordinates ([Morse and Feshbach, 1953](#)). Also, the boundary densities are expanded by using the eigenfunction expansion in companion with a Jacobian term. The advantage of free of calculating principal value is gained. Following the successful experience of the annular case ([Chen et al., 2003](#)), we extend to the elliptical case in this paper. In order to analytically verify the occurring mechanism of the spurious eigenvalues for multiply-connected problem containing elliptical boundaries, the confocal elliptical membrane is considered. The boundary element method is also implemented to demonstrate the finding by using the present approach. Furthermore, the commercial finite-element code ABAQUS is also utilized to provide eigensolutions for comparisons. As mentioned above, it is already known in the literature by [Kobayashi and Nishimura \(1982\)](#) that spurious eigensolutions depend on the geometry of inner boundary and the approach used. However, all the related efforts were focused on eigenproblems involving circular boundaries. Spurious eigenvalue of a confocal elliptical membrane have not been analytically studied in detail by using the BIEM to the authors' best knowledge. Accordingly, this paper is focused on analytically deriving the true and spurious eigenequations of a confocal elliptical membrane by using the BIEM. Finally, we also employ CHIEF method, the SVD updating technique and the Burton & Miller approach to suppress the spurious appearance of eigenvalues.

## 2. Problem statement and the present approach

### 2.1. Problem statement

For the eigenproblem of a multiply-connected membrane, the governing equation is the Helmholtz equation as follows:

$$(\nabla^2 + k^2)u(\mathbf{x}) = 0, \quad \mathbf{x} \in D, \quad (1)$$

where  $\nabla^2$  is the Laplacian operator,  $k$  is the wave number,  $u(\mathbf{x})$  is the displacement of the membrane,  $\mathbf{x}$  is the field point and  $D$  is the domain of interest.

### 2.2. Dual boundary integral formulations – the conventional version

Based on the Green's third identity, the dual boundary integral equations for the domain point are shown below:

$$2\pi u(\mathbf{x}) = \int_B T(\mathbf{s}, \mathbf{x})u(\mathbf{s})dB(\mathbf{s}) - \int_B U(\mathbf{s}, \mathbf{x})t(\mathbf{s})dB(\mathbf{s}), \quad \mathbf{x} \in D, \quad (2)$$

$$2\pi t(\mathbf{x}) = \int_B M(\mathbf{s}, \mathbf{x})u(\mathbf{s})dB(\mathbf{s}) - \int_B L(\mathbf{s}, \mathbf{x})t(\mathbf{s})dB(\mathbf{s}), \quad \mathbf{x} \in D, \quad (3)$$

where  $\mathbf{s}$  is the source point,  $B$  is the boundary of membrane,  $t$  is the normal derivative of displacement and  $U(\mathbf{s}, \mathbf{x})$  is the fundamental function which satisfies

$$(\nabla^2 + k^2)U(\mathbf{s}, \mathbf{x}) = 2\pi\delta(\mathbf{x} - \mathbf{s}), \quad (4)$$

where  $\delta$  is the Dirac-delta function. The other kernel functions  $T(\mathbf{s}, \mathbf{x})$ ,  $L(\mathbf{s}, \mathbf{x})$  and  $M(\mathbf{s}, \mathbf{x})$  are defined by

$$T(\mathbf{s}, \mathbf{x}) = \frac{\partial U(\mathbf{s}, \mathbf{x})}{\partial n_{\mathbf{s}}}, \quad (5)$$

$$L(\mathbf{s}, \mathbf{x}) = \frac{\partial U(\mathbf{s}, \mathbf{x})}{\partial n_{\mathbf{x}}}, \quad (6)$$

$$M(\mathbf{s}, \mathbf{x}) = \frac{\partial^2 U(\mathbf{s}, \mathbf{x})}{\partial n_{\mathbf{s}} \partial n_{\mathbf{x}}}, \quad (7)$$

where  $n_{\mathbf{x}}$  and  $n_{\mathbf{s}}$  denote the unit outward normal vector at the field point and the source point, respectively. By moving the field point  $\mathbf{x}$  to the boundary which is smooth, the dual boundary integral equations for the boundary point can be obtained as follows:

$$\begin{aligned} \pi u(\mathbf{x}) &= C.P.V. \int_B T(\mathbf{s}, \mathbf{x})u(\mathbf{s})dB(\mathbf{s}) \\ &\quad - R.P.V. \int_B U(\mathbf{s}, \mathbf{x})t(\mathbf{s})dB(\mathbf{s}), \quad \mathbf{x} \in B, \end{aligned} \quad (8)$$

$$\begin{aligned} \pi t(\mathbf{x}) &= H.P.V. \int_B M(\mathbf{s}, \mathbf{x})u(\mathbf{s})dB(\mathbf{s}) \\ &\quad - C.P.V. \int_B L(\mathbf{s}, \mathbf{x})t(\mathbf{s})dB(\mathbf{s}), \quad \mathbf{x} \in B, \end{aligned} \quad (9)$$

$$U(\mathbf{s}, \mathbf{x}) = \begin{cases} -2\pi i \left( \sum_{m=0}^{\infty} \left[ \frac{Se_m(q, \eta_{\mathbf{s}})}{M_m^e(q)} \right] Se_m(q, \eta_{\mathbf{x}}) Je_m(q, \xi_{\mathbf{s}}) He_m(q, \xi_{\mathbf{x}}) + \sum_{m=1}^{\infty} \left[ \frac{So_m(q, \eta_{\mathbf{s}})}{M_m^o(q)} \right] So_m(q, \eta_{\mathbf{x}}) Jo_m(q, \xi_{\mathbf{s}}) Ho_m(q, \xi_{\mathbf{x}}) \right), & \xi_{\mathbf{x}} \geq \xi_{\mathbf{s}}, \\ -2\pi i \left( \sum_{m=0}^{\infty} \left[ \frac{Se_m(q, \eta_{\mathbf{s}})}{M_m^e(q)} \right] Se_m(q, \eta_{\mathbf{x}}) Je_m(q, \xi_{\mathbf{x}}) He_m(q, \xi_{\mathbf{s}}) + \sum_{m=1}^{\infty} \left[ \frac{So_m(q, \eta_{\mathbf{s}})}{M_m^o(q)} \right] So_m(q, \eta_{\mathbf{x}}) Jo_m(q, \xi_{\mathbf{x}}) Ho_m(q, \xi_{\mathbf{s}}) \right), & \xi_{\mathbf{x}} < \xi_{\mathbf{s}}, \end{cases} \quad (17)$$

where  $R.P.V.$ ,  $C.P.V.$  and  $H.P.V.$  denote the Riemann principal value (Riemann sum), Cauchy principal value and Hadamard (or so-called Mangler) principal value, respectively. By collocating the field point  $\mathbf{x}$  on the complementary domain, we obtain the dual null-field boundary integral equations as shown below:

$$0 = \int_B T(\mathbf{s}, \mathbf{x})u(\mathbf{s})dB(\mathbf{s}) - \int_B U(\mathbf{s}, \mathbf{x})t(\mathbf{s})dB(\mathbf{s}), \quad \mathbf{x} \in D^c, \quad (10)$$

$$0 = \int_B M(\mathbf{s}, \mathbf{x})u(\mathbf{s})dB(\mathbf{s}) - \int_B L(\mathbf{s}, \mathbf{x})t(\mathbf{s})dB(\mathbf{s}), \quad \mathbf{x} \in D^c, \quad (11)$$

where  $D^c$  denote the complementary domain.

### 2.3. Dual boundary integral formulations – the present version

By introducing the separable kernels, the collocation point in Eqs. (2), (3), (10) and (11) can be located on the real boundary without need of calculating principal value. Therefore, the dual BIE and dual null-field BIE can be rewritten in two parts as given in the following formulation of Eqs. (12) and (14), instead of three parts using Eqs. (2), (8) and (10) in the conventional BEM

$$2\pi u(\mathbf{x}) = \int_B T(\mathbf{s}, \mathbf{x})u(\mathbf{s})dB(\mathbf{s}) - \int_B U(\mathbf{s}, \mathbf{x})t(\mathbf{s})dB(\mathbf{s}), \quad \mathbf{x} \in D \cup B, \quad (12)$$

$$2\pi t(\mathbf{x}) = \int_B M(\mathbf{s}, \mathbf{x})u(\mathbf{s})dB(\mathbf{s}) - \int_B L(\mathbf{s}, \mathbf{x})t(\mathbf{s})dB(\mathbf{s}), \quad \mathbf{x} \in D \cup B, \quad (13)$$

and

$$0 = \int_B T(\mathbf{s}, \mathbf{x})u(\mathbf{s})dB(\mathbf{s}) - \int_B U(\mathbf{s}, \mathbf{x})t(\mathbf{s})dB(\mathbf{s}), \quad \mathbf{x} \in D^c \cup B, \quad (14)$$

$$0 = \int_B M(\mathbf{s}, \mathbf{x})u(\mathbf{s})dB(\mathbf{s}) - \int_B L(\mathbf{s}, \mathbf{x})t(\mathbf{s})dB(\mathbf{s}), \quad \mathbf{x} \in D^c \cup B. \quad (15)$$

It is noted that Eqs. (12)–(15) can contain the boundary point ( $\mathbf{x} \rightarrow B$ ) since the kernel functions ( $U, T, L$  and  $M$ ) are expressed in terms of various separable kernels which will be elaborated on later in Eqs. (17) and (25)–(27).

### 2.4. Expansions of fundamental solution and boundary density using the elliptic coordinates

The closed-form fundamental solution as previously mentioned is

$$U(\mathbf{s}, \mathbf{x}) = -\frac{i\pi H_0^{(1)}(kr)}{2}, \quad (16)$$

where  $r \equiv |\mathbf{s} - \mathbf{x}|$  is the distance between the source point and the field point,  $i$  is the imaginary number with  $i^2 = -1$  and  $H_0^{(1)}$  is the zeroth-order Hankel function of the first kind. To fully utilize the property of elliptical geometry, the separable kernel and eigenfunction expansion are utilized for the analytical integration of boundary integrals. In the elliptic coordinates, the field point  $\mathbf{x}$  and source point  $\mathbf{s}$  can be expressed as  $\mathbf{x} = (\xi_{\mathbf{x}}, \eta_{\mathbf{x}})$  and  $\mathbf{s} = (\xi_{\mathbf{s}}, \eta_{\mathbf{s}})$ , respectively. The fundamental solution,  $U(\mathbf{s}, \mathbf{x})$ , can be expanded in terms of separable kernel as shown below:

$$q = (ck/2)^2, \quad (18)$$

where  $c$  is the half distance between two foci,  $Se_m$  and  $So_m$  are the  $m$ th-order even and odd Mathieu functions (angular Mathieu

functions), respectively,  $Je_m$  and  $Jo_m$  are the  $m$ th-order even and odd modified Mathieu functions (radial Mathieu functions) of the first kind, respectively,  $He_m$  and  $Ho_m$  are the even and odd  $m$ th-order modified Mathieu functions (Mathieu-Hankel functions) of the third kind, respectively and are defined as

$$He_m(q, \xi) = Je_m(q, \xi) + iYe_m(q, \xi), \quad (19)$$

$$Ho_m(q, \xi) = Jo_m(q, \xi) + iYo_m(q, \xi), \quad (20)$$

in which,  $Ye_m$  and  $Yo_m$  are the  $m$ th-order even and odd modified Mathieu functions of the second kind, respectively,  $M_m^e$  and  $M_m^o$  are the normalized constants for the norm of angular Mathieu function and can be determined by

$$M_m^e(q) = \int_{-\pi}^{\pi} (Se_m(q, \eta))^2 d\eta = \pi, \quad (21)$$

$$M_m^o(q) = \int_{-\pi}^{\pi} (So_m(q, \eta))^2 d\eta = \pi. \quad (22)$$

The contour plots of the closed-form fundamental solution and the separable kernel by using Eqs. (16) and (17), respectively, are shown in Table 1. After comparing with the two different representations, the closed-form fundamental solution (Eq. (16)) and separable kernel (Eq. (17)), agreement is made. The normal derivative on the boundary point along the elliptic curve in terms of the elliptic coordinates is defined by

$$t(\mathbf{x}) = \frac{\partial u(\mathbf{x})}{\partial n_{\mathbf{x}}} = \frac{1}{J_{\mathbf{x}}} \frac{\partial u(\mathbf{x})}{\partial \xi_{\mathbf{x}}}, \quad \mathbf{x} \in B, \quad (23)$$

where  $J_{\mathbf{x}}$  is the Jacobian term of the field point  $\mathbf{x}$  as shown below:

$$J_{\mathbf{x}} = c\sqrt{(\sinh(\xi_{\mathbf{x}}) \cos(\eta_{\mathbf{x}}))^2 + (\cosh(\xi_{\mathbf{x}}) \sin(\eta_{\mathbf{x}}))^2}. \quad (24)$$

Then, the other kernel functions,  $T(\mathbf{s}, \mathbf{x})$ ,  $L(\mathbf{s}, \mathbf{x})$  and  $M(\mathbf{s}, \mathbf{x})$  can be obtained by using Eqs. (5)–(7) as shown below:

$$T(\mathbf{s}, \mathbf{x}) = \begin{cases} -2\pi i \frac{1}{J_{\mathbf{s}}} \left( \sum_{m=0}^{\infty} \left[ \frac{Se_m(q, \eta_{\mathbf{s}})}{M_m^e(q)} \right] Se_m(q, \eta_{\mathbf{x}}) Je'_m(q, \xi_{\mathbf{s}}) He_m(q, \xi_{\mathbf{x}}) + \sum_{m=1}^{\infty} \left[ \frac{So_m(q, \eta_{\mathbf{s}})}{M_m^o(q)} \right] So_m(q, \eta_{\mathbf{x}}) Jo'_m(q, \xi_{\mathbf{s}}) Ho_m(q, \xi_{\mathbf{x}}) \right), & \xi_{\mathbf{x}} > \xi_{\mathbf{s}}, \\ -2\pi i \frac{1}{J_{\mathbf{s}}} \left( \sum_{m=0}^{\infty} \left[ \frac{Se_m(q, \eta_{\mathbf{s}})}{M_m^e(q)} \right] Se_m(q, \eta_{\mathbf{x}}) Je_m(q, \xi_{\mathbf{x}}) He'_m(q, \xi_{\mathbf{s}}) + \sum_{m=1}^{\infty} \left[ \frac{So_m(q, \eta_{\mathbf{s}})}{M_m^o(q)} \right] So_m(q, \eta_{\mathbf{x}}) Jo_m(q, \xi_{\mathbf{x}}) Ho'_m(q, \xi_{\mathbf{s}}) \right), & \xi_{\mathbf{x}} < \xi_{\mathbf{s}}, \end{cases} \quad (25)$$

$$L(\mathbf{s}, \mathbf{x}) = \begin{cases} -2\pi i \frac{1}{J_{\mathbf{x}}} \left( \sum_{m=0}^{\infty} \left[ \frac{Se_m(q, \eta_{\mathbf{s}})}{M_m^e(q)} \right] Se_m(q, \eta_{\mathbf{x}}) Je_m(q, \xi_{\mathbf{s}}) He'_m(q, \xi_{\mathbf{x}}) + \sum_{m=1}^{\infty} \left[ \frac{So_m(q, \eta_{\mathbf{s}})}{M_m^o(q)} \right] So_m(q, \eta_{\mathbf{x}}) Jo_m(q, \xi_{\mathbf{s}}) Ho'_m(q, \xi_{\mathbf{x}}) \right), & \xi_{\mathbf{x}} > \xi_{\mathbf{s}}, \\ -2\pi i \frac{1}{J_{\mathbf{x}}} \left( \sum_{m=0}^{\infty} \left[ \frac{Se_m(q, \eta_{\mathbf{s}})}{M_m^e(q)} \right] Se_m(q, \eta_{\mathbf{x}}) Je'_m(q, \xi_{\mathbf{x}}) He_m(q, \xi_{\mathbf{s}}) + \sum_{m=1}^{\infty} \left[ \frac{So_m(q, \eta_{\mathbf{s}})}{M_m^o(q)} \right] So_m(q, \eta_{\mathbf{x}}) Jo'_m(q, \xi_{\mathbf{x}}) Ho_m(q, \xi_{\mathbf{s}}) \right), & \xi_{\mathbf{x}} < \xi_{\mathbf{s}}, \end{cases} \quad (26)$$

$$M(\mathbf{s}, \mathbf{x}) = \begin{cases} -2\pi i \frac{1}{J_{\mathbf{s}} J_{\mathbf{x}}} \left( \sum_{m=0}^{\infty} \left[ \frac{Se_m(q, \eta_{\mathbf{s}})}{M_m^e(q)} \right] Se_m(q, \eta_{\mathbf{x}}) Je'_m(q, \xi_{\mathbf{s}}) He'_m(q, \xi_{\mathbf{x}}) + \sum_{m=1}^{\infty} \left[ \frac{So_m(q, \eta_{\mathbf{s}})}{M_m^o(q)} \right] So_m(q, \eta_{\mathbf{x}}) Jo'_m(q, \xi_{\mathbf{s}}) Ho'_m(q, \xi_{\mathbf{x}}) \right), & \xi_{\mathbf{x}} \geq \xi_{\mathbf{s}}, \\ -2\pi i \frac{1}{J_{\mathbf{s}} J_{\mathbf{x}}} \left( \sum_{m=0}^{\infty} \left[ \frac{Se_m(q, \eta_{\mathbf{s}})}{M_m^e(q)} \right] Se_m(q, \eta_{\mathbf{x}}) Je'_m(q, \xi_{\mathbf{x}}) He'_m(q, \xi_{\mathbf{s}}) + \sum_{m=1}^{\infty} \left[ \frac{So_m(q, \eta_{\mathbf{s}})}{M_m^o(q)} \right] So_m(q, \eta_{\mathbf{x}}) Jo'_m(q, \xi_{\mathbf{x}}) Ho'_m(q, \xi_{\mathbf{s}}) \right), & \xi_{\mathbf{x}} < \xi_{\mathbf{s}}, \end{cases} \quad (27)$$

where  $J_{\mathbf{s}}$  is the Jacobian term of the source point,  $\mathbf{s}$ , as shown below:

$$J_{\mathbf{s}} = c\sqrt{(\sinh(\xi_{\mathbf{s}}) \cos(\eta_{\mathbf{s}}))^2 + (\cosh(\xi_{\mathbf{s}}) \sin(\eta_{\mathbf{s}}))^2}. \quad (28)$$

It is noted that  $U(\mathbf{s}, \mathbf{x})$ , and  $M(\mathbf{s}, \mathbf{x})$  kernels in Eqs. (17) and (27), respectively, contain the equal sign of  $\xi_{\mathbf{x}} = \xi_{\mathbf{s}}$ . Since the potential result from  $T(\mathbf{s}, \mathbf{x})$ , and  $L(\mathbf{s}, \mathbf{x})$  kernels are discontinuous across the boundary, the potentials of  $T(\mathbf{s}, \mathbf{x})$ , and  $L(\mathbf{s}, \mathbf{x})$  kernels for  $\xi_{\mathbf{x}} \rightarrow \xi_{\mathbf{s}}^+$  and  $\xi_{\mathbf{x}} \rightarrow \xi_{\mathbf{s}}^-$  are different. This is the reason why  $\xi_{\mathbf{x}} = \xi_{\mathbf{s}}$  is not included in the separable kernels of  $T(\mathbf{s}, \mathbf{x})$ , and  $L(\mathbf{s}, \mathbf{x})$  kernels in

Eqs. (25) and (26), respectively. The orthogonal relations of the angular Mathieu functions are shown below:

$$\int_{-\pi}^{\pi} Se_m(q, \eta) Se_n(q, \eta) d\eta = \begin{cases} \pi, & m = n, \\ 0, & m \neq n, \end{cases} \quad (29)$$

$$\int_{-\pi}^{\pi} So_m(q, \eta) So_n(q, \eta) d\eta = \begin{cases} \pi, & m = n, \\ 0, & m \neq n, \end{cases} \quad (30)$$

$$\int_{-\pi}^{\pi} Se_m(q, \eta) So_n(q, \eta) d\eta = 0. \quad (31)$$

In order to fully utilize the orthogonal relations of the angular Mathieu functions, we apply the eigenfunction expansion to approximate the unknown boundary densities. The displacement,  $u(\mathbf{s})$ , and its normal derivative,  $t(\mathbf{s}) = \frac{1}{J_{\mathbf{s}}} \frac{\partial u(\mathbf{s})}{\partial \xi_{\mathbf{s}}}$  along the elliptical boundary, can be adaptively expressed as

$$u(\mathbf{s}) = \sum_{n=0}^{\infty} g_n Se_n(q, \eta_{\mathbf{s}}) + \sum_{n=1}^{\infty} h_n So_n(q, \eta_{\mathbf{s}}), \quad \mathbf{s} \in B, \quad (32)$$

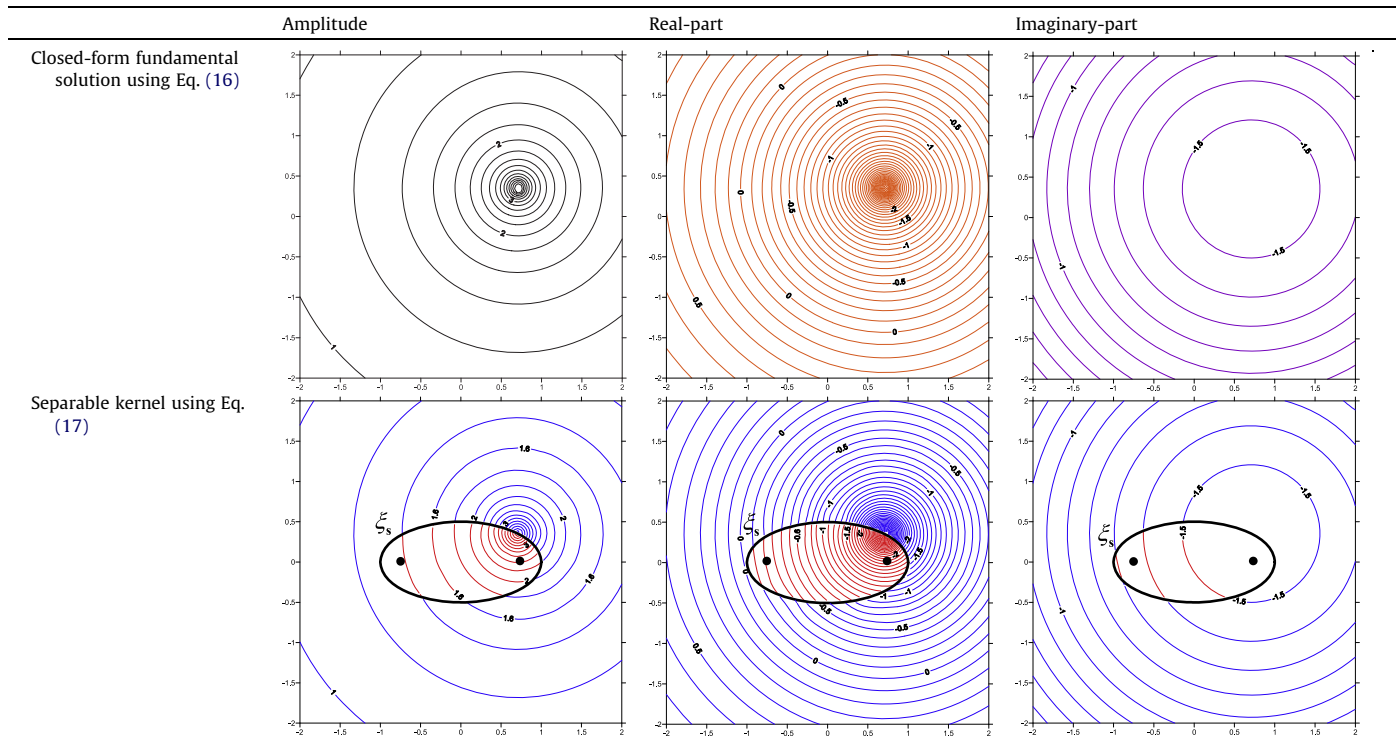
$$t(\mathbf{s}) = \frac{1}{J_{\mathbf{s}}} \left( \sum_{n=0}^{\infty} p_n Se_n(q, \eta_{\mathbf{s}}) + \sum_{n=1}^{\infty} q_n So_n(q, \eta_{\mathbf{s}}) \right), \quad \mathbf{s} \in B, \quad (33)$$

respectively, where  $g_n$ ,  $h_n$ ,  $p_n$  and  $q_n$  are the unknown coefficients of the eigenfunctions. The Jacobian term  $J_{\mathbf{s}}$  may appear either in the kernel functions of Eqs. (25)–(27), the boundary densities of Eq. (33) or the elliptical boundary contour integration ( $dB(\mathbf{s}) = J_{\mathbf{s}} d\eta_{\mathbf{s}}$ ). We may worry about the possible failure of orthogonal relations for the Mathieu bases due to the presence of  $J_{\mathbf{s}}$ . Fortunately, the Jacobian terms can be cancelled each other out. Therefore, the orthogonal relations can be fully utilized in the contour integration of elliptical boundary and boundary integrals can be analytically determined.

### 3. Analytical derivations for true and spurious eigensolutions of a confocal elliptical membrane using the separable kernels

Following successful experiences in annular membranes (Chen et al., 2001, 2003), it has been revealed that the corresponding mechanism of the spurious eigensolutions of the multiply-connected problem containing circular boundaries depends on the geometry of inner boundary and the integral formulation. Now, we extend to study elliptical cases by using Eqs. (14) and (15) in conjunction with the elliptic coordinates and the Mathieu functions. A confocal elliptical membrane is considered as shown in Fig. 1. In order to analytically study the problem, the same half



**Table 1**Sketch of contour plots of the closed-form fundamental solution and the separable kernel ( $k = 0.4$ ,  $\eta_s = \frac{\pi}{4}$ ,  $a = 1$ ,  $b = 0.5$ ).

distance between two foci is used, i.e., the parameters of the confocal elliptical membrane are  $\xi = \xi_0$  and  $\xi = \xi_1$  for outer and inner boundaries, respectively. The confocal membrane is subject to fixed-fixed B.C. as shown below:

$$u(\mathbf{x}) = 0, \quad \mathbf{x} \in B_0 \cup B_1, \quad (34)$$

Eqs. (14) and (15) are written as

$$0 = \sum_{j=0}^1 \int_{B_j} U(\mathbf{s}_j, \mathbf{x}) t(\mathbf{s}_j) dB(\mathbf{s}_j), \quad \mathbf{x} \in D^c \cup B, \quad (35)$$

$$0 = \sum_{j=0}^1 \int_{B_j} L(\mathbf{s}_j, \mathbf{x}) t(\mathbf{s}_j) dB(\mathbf{s}_j), \quad \mathbf{x} \in D^c \cup B, \quad (36)$$

and boundary densities are expressed by

$$t_0(\mathbf{s}) = \frac{1}{J_s} \left( \sum_{n=0}^{\infty} p_n^0 S e_n(q, \eta_s) + \sum_{n=1}^{\infty} q_n^0 S o_n(q, \eta_s) \right), \quad \mathbf{s} \in B_0, \quad (37)$$

$$t_1(\mathbf{s}) = \frac{1}{J_s} \left( \sum_{n=0}^{\infty} p_n^1 S e_n(q, \eta_s) + \sum_{n=1}^{\infty} q_n^1 S o_n(q, \eta_s) \right), \quad \mathbf{s} \in B_1, \quad (38)$$

where  $p_n^j$  and  $q_n^j$  are the unknown coefficients of the eigenfunctions on  $B_j$  ( $j = 0, 1$ ). Substituting Eqs. (37) and (38) to Eq. (35) and collocating the field point exactly on the outer boundary  $B_0$ , we have

$$\begin{aligned} & -2\pi i \left( \sum_{m=0}^{\infty} p_m^0 S e_m(q, \eta) J e_m(q, \xi_0) H e_m(q, \xi_0) \right. \\ & + \sum_{m=1}^{\infty} q_m^0 S o_m(q, \eta) J o_m(q, \xi_0) H o_m(q, \xi_0) \\ & + \sum_{m=0}^{\infty} p_m^1 S e_m(q, \eta) J e_m(q, \xi_1) H e_m(q, \xi_0) \\ & \left. + \sum_{m=1}^{\infty} q_m^1 S o_m(q, \eta) J o_m(q, \xi_1) H o_m(q, \xi_0) \right) = 0. \end{aligned} \quad (39)$$

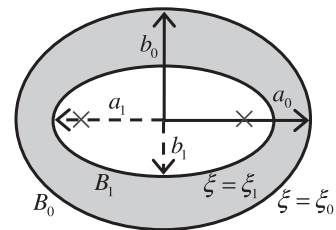
By collocating the field point of Eq. (35) exactly on the inner boundary  $B_1$ , we have

$$\begin{aligned} & -2\pi i \left( \sum_{m=0}^{\infty} p_m^0 S e_m(q, \eta) J e_m(q, \xi_1) H e_m(q, \xi_0) \right. \\ & + \sum_{m=1}^{\infty} q_m^0 S o_m(q, \eta) J o_m(q, \xi_1) H o_m(q, \xi_0) \\ & + \sum_{m=0}^{\infty} p_m^1 S e_m(q, \eta) J e_m(q, \xi_1) H e_m(q, \xi_1) \\ & \left. + \sum_{m=1}^{\infty} q_m^1 S o_m(q, \eta) J o_m(q, \xi_1) H o_m(q, \xi_1) \right) = 0. \end{aligned} \quad (40)$$

According to Eqs. (39) and (40), we obtain the relation between  $p_m^0$ ,  $q_m^0$  and  $p_m^1$ ,  $q_m^1$  as follows:

$$p_m^0 = -\frac{J e_m(q, \xi_1) H e_m(q, \xi_0)}{J e_m(q, \xi_0) H e_m(q, \xi_0)} p_m^1, \quad m = 0, 1, 2, \dots, \quad (41)$$

$$q_m^0 = -\frac{J o_m(q, \xi_1) H o_m(q, \xi_0)}{J o_m(q, \xi_0) H o_m(q, \xi_0)} q_m^1, \quad m = 1, 2, \dots, \quad (42)$$



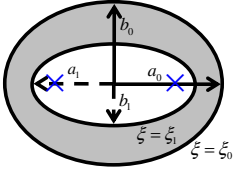
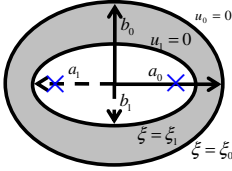
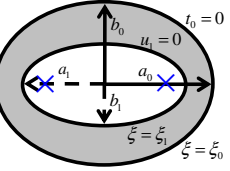
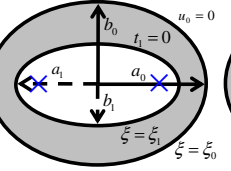
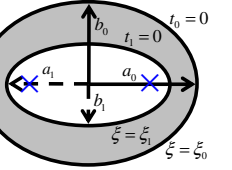
(a)  $u(\mathbf{x}) = 0, \mathbf{x} \in B_0 \cup B_1$

(b)  $t(\mathbf{x}) = 0, \mathbf{x} \in B_0 \cup B_1$

**Fig. 1.** A confocal elliptical membrane.

**Table 2**

True and spurious eigenequations for the confocal elliptical annulus subject to various boundary conditions.

| Figure sketch   |                        | (Fixed-fixed)   | (Free-fixed)  | (Fixed-free)  | (Free-free)   |
|---|------------------------|---|---|---|---|
|  |                        |    |   |    |    |
| UT Eq. (14)   | True eigenequation     | $J e_m(q, \xi_0) Y e_m(q, \xi_1) - J e_m(q, \xi_1) Y e_m(q, \xi_0) = 0$   | $J e'_m(q, \xi_0) Y e_m(q, \xi_1) - J e_m(q, \xi_1) Y e'_m(q, \xi_0) = 0$   | $J e_m(q, \xi_0) Y e'_m(q, \xi_1) - J e'_m(q, \xi_1) Y e_m(q, \xi_0) = 0$   | $J e'_m(q, \xi_0) Y e'_m(q, \xi_1) - J e'_m(q, \xi_1) Y e'_m(q, \xi_0) = 0$   |
|   | Spurious eigenequation | $J o_m(q, \xi_0) Y o_m(q, \xi_1) - J o_m(q, \xi_1) Y o_m(q, \xi_0) = 0$ $J_m(kr_0) Y_m(kr_1) - J_m(kr_1) Y_m(kr_0) = 0 \text{ (annular case)}$  | $J o'_m(q, \xi_0) Y o_m(q, \xi_1) - J o_m(q, \xi_1) Y o'_m(q, \xi_0) = 0$ $J'_m(kr_0) Y_m(kr_1) - J_m(kr_1) Y'_m(kr_0) = 0 \text{ (annular case)}$  | $J o_m(q, \xi_0) Y o'_m(q, \xi_1) - J o'_m(q, \xi_1) Y o_m(q, \xi_0) = 0$ $J_m(kr_0) Y'_m(kr_1) - J'_m(kr_1) Y_m(kr_0) = 0 \text{ (annular case)}$  | $J o'_m(q, \xi_0) Y o'_m(q, \xi_1) - J o'_m(q, \xi_1) Y o'_m(q, \xi_0) = 0$ $J'_m(kr_0) Y'_m(kr_1) - J'_m(kr_1) Y'_m(kr_0) = 0 \text{ (annular case)}$  |
|   |                        | $J e_m(q, \xi_1) = 0$ $J o_m(q, \xi_1) = 0$   | $J e_m(q, \xi_1) = 0$ $J o_m(q, \xi_1) = 0$   | $J e_m(q, \xi_1) = 0$ $J o_m(q, \xi_1) = 0$   | $J e_m(q, \xi_1) = 0$ $J o_m(q, \xi_1) = 0$   |
|   |                        | $J_m(kr_1) = 0 \text{ (annular case)}$  | $J_m(kr_1) = 0 \text{ (annular case)}$  | $J_m(kr_1) = 0 \text{ (annular case)}$  | $J_m(kr_1) = 0 \text{ (annular case)}$  |
| LM Eq. (15)   | True eigenequation     | $J e_m(q, \xi_0) Y e_m(q, \xi_1) - J e_m(q, \xi_1) Y e_m(q, \xi_0) = 0$ $J o_m(q, \xi_0) Y o_m(q, \xi_1) - J o_m(q, \xi_1) Y o_m(q, \xi_0) = 0$ | $J e'_m(q, \xi_0) Y e_m(q, \xi_1) - J e_m(q, \xi_1) Y e'_m(q, \xi_0) = 0$ $J o'_m(q, \xi_0) Y o_m(q, \xi_1) - J o_m(q, \xi_1) Y o'_m(q, \xi_0) = 0$ | $J e_m(q, \xi_0) Y e'_m(q, \xi_1) - J e'_m(q, \xi_1) Y e_m(q, \xi_0) = 0$ $J o_m(q, \xi_0) Y o'_m(q, \xi_1) - J o'_m(q, \xi_1) Y o_m(q, \xi_0) = 0$ | $J e'_m(q, \xi_0) Y e'_m(q, \xi_1) - J e'_m(q, \xi_1) Y e'_m(q, \xi_0) = 0$ $J o'_m(q, \xi_0) Y o'_m(q, \xi_1) - J o'_m(q, \xi_1) Y o'_m(q, \xi_0) = 0$ |
|   | Spurious eigenequation | $J e'_m(q, \xi_1) = 0$ $J o'_m(q, \xi_1) = 0$   | $J e'_m(q, \xi_1) = 0$ $J o'_m(q, \xi_1) = 0$   | $J e'_m(q, \xi_1) = 0$ $J o'_m(q, \xi_1) = 0$   | $J e'_m(q, \xi_1) = 0$ $J o'_m(q, \xi_1) = 0$   |
|   |                        | $J'_m(kr_1) = 0 \text{ (annular case)}$   | $J'_m(kr_1) = 0 \text{ (annular case)}$   | $J'_m(kr_1) = 0 \text{ (annular case)}$   | $J'_m(kr_1) = 0 \text{ (annular case)}$   |

and

$$p_m^0 = -\frac{J e_m(q, \xi_1) H e_m(q, \xi_1)}{J e_m(q, \xi_1) H e_m(q, \xi_0)} p_m^1, \quad m = 0, 1, 2, \dots, \quad (43)$$

$$q_m^0 = -\frac{J o_m(q, \xi_1) H o_m(q, \xi_1)}{J o_m(q, \xi_1) H o_m(q, \xi_0)} q_m^1, \quad m = 1, 2, \dots, \quad (44)$$

respectively. Combining Eqs. (41)–(44), we obtain four possible eigenequations,

$$J e_m(q, \xi_0) Y e_m(q, \xi_1) - J e_m(q, \xi_1) Y e_m(q, \xi_0) = 0, \quad m = 0, 1, 2, \dots, \quad (45)$$

$$J o_m(q, \xi_0) Y o_m(q, \xi_1) - J o_m(q, \xi_1) Y o_m(q, \xi_0) = 0, \quad m = 1, 2, \dots, \quad (46)$$

$$J e_m(q, \xi_1) = 0, \quad m = 0, 1, 2, \dots, \quad (47)$$

$$J o_m(q, \xi_1) = 0, \quad m = 1, 2, \dots \quad (48)$$

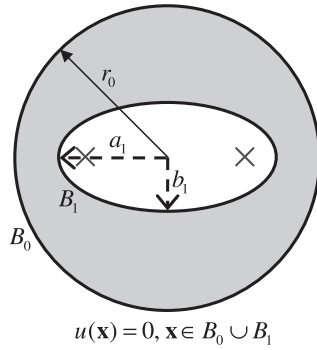


Fig. 2. A circular membrane containing an elliptical hole.

Based on Eq. (36), we obtain four possible eigenequations. Namely, the following two equations

$$J e'_m(q, \xi_1) = 0, \quad m = 0, 1, 2, \dots, \quad (49)$$

$$J o'_m(q, \xi_1) = 0, \quad m = 1, 2, \dots, \quad (50)$$

and the other two are the same with Eqs. (45) and (46). If we employ two different approaches to solve the same problem, we should obtain the same true solution. Therefore, it indicates that Eqs. (47), (48) and Eqs. (49), (50) are the spurious eigenequations by using Eqs. (35) and (36), respectively. The true and spurious eigenequations for problems with various boundary conditions (free–fixed, fixed–free and free–free) are shown in Table 2. It is interesting to find that spurious eigenequations depend on the geometry of inner boundary and the approach used. This conclusion agrees well with that of the annular case (Chen et al., 2001, 2003).

#### 4. Numerical detection of true and spurious eigenvalues using the conventional dual BEMs in conjunction with the SVD technique

In order to demonstrate the validity of the analytical solution by using the BIEM, we employ the BEM for comparisons. By employing the constant element scheme and moving the field point  $\mathbf{x}$

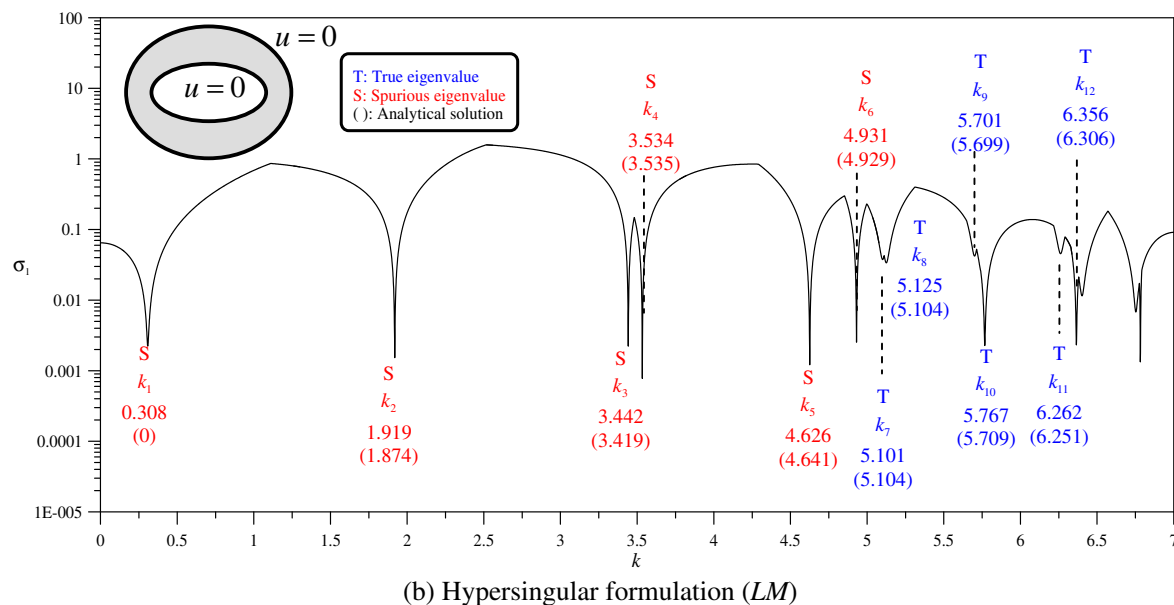
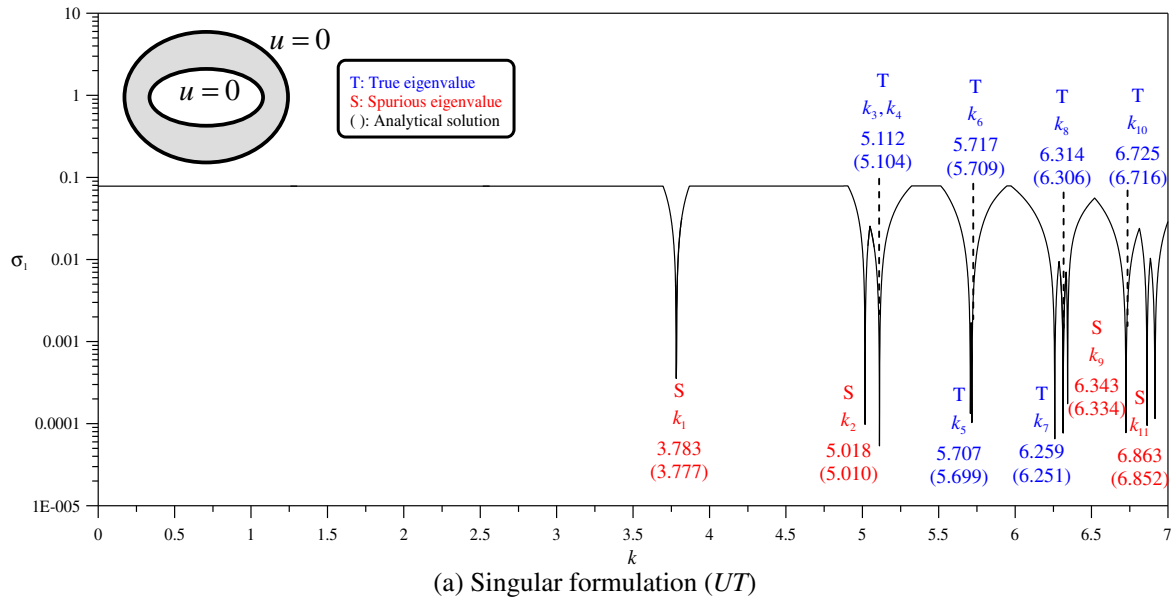


Fig. 3. Detection of possible eigenvalues for the fixed–fixed confocal elliptical membrane by plotting the minimum singular value  $\sigma_1$  versus  $k$  in the BEM.

**Table 3**

The former ten possible eigenvalues of a confocal elliptical membrane subject to the fixed–fixed boundary condition by using the singular BIEM/BEM and FEM.

| Method                       | Eigenvalue |         |       |       |       |       |       |       |         |          |
|------------------------------|------------|---------|-------|-------|-------|-------|-------|-------|---------|----------|
|                              | $k_1$      | $k_2$   | $k_3$ | $k_4$ | $k_5$ | $k_6$ | $k_7$ | $k_8$ | $k_9$   | $k_{10}$ |
| Present method               | (3.777)    | (5.010) | 5.104 | 5.104 | 5.699 | 5.709 | 6.251 | 6.306 | (6.334) | 6.716    |
| BEM(No. elements = 100)      | (3.783)    | (5.018) | 5.112 | 5.112 | 5.707 | 5.717 | 6.259 | 6.314 | (6.343) | 6.725    |
| ABAQUS (No. elements = 2460) | –          | –       | 5.104 | 5.104 | 5.699 | 5.709 | 6.251 | 6.306 | –       | 6.716    |

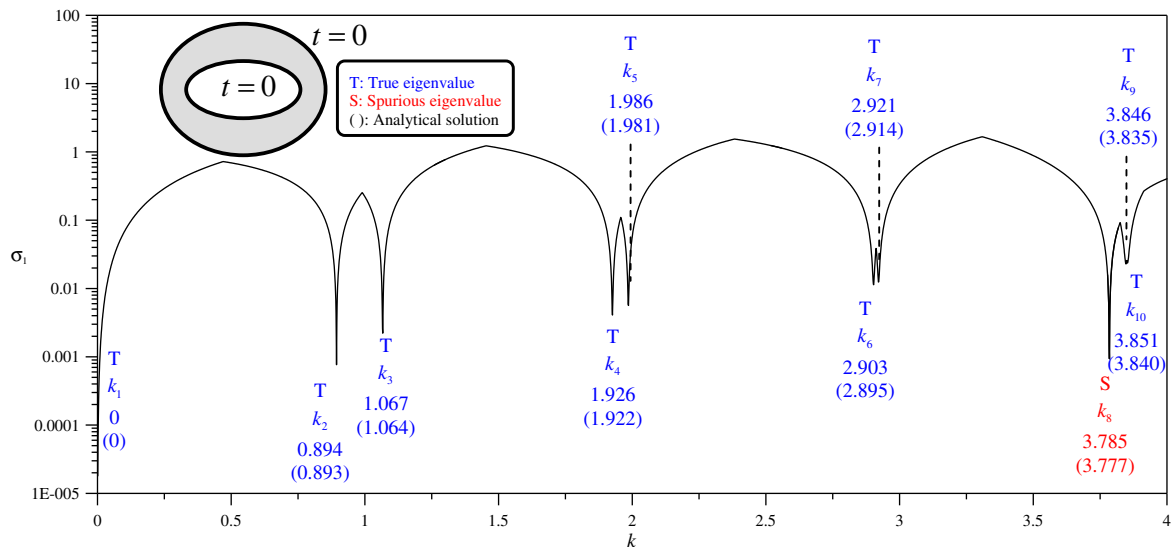
Note: The data inside the parentheses denote the spurious eigenvalue, which relates to the zeros of the  $m$ th-order (even or odd) modified Mathieu functions of the first kind, ( $Je_m(q, \xi_1)$  or  $Jo_m(q, \xi_1)$ ).

**Table 4**

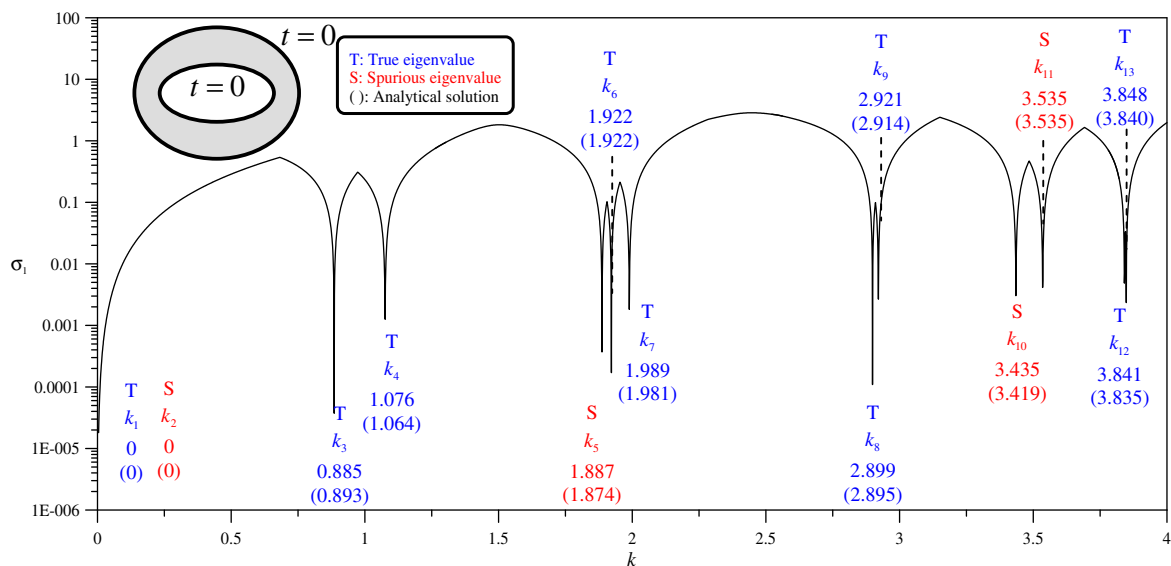
The former ten possible eigenvalues of a confocal elliptical membrane subject to the fixed–fixed boundary condition by using the hypersingular BIEM/BEM and FEM.

| Method                       | Eigenvalue |         |         |         |         |         |       |       |       |          |
|------------------------------|------------|---------|---------|---------|---------|---------|-------|-------|-------|----------|
|                              | $k_1$      | $k_2$   | $k_3$   | $k_4$   | $k_5$   | $k_6$   | $k_7$ | $k_8$ | $k_9$ | $k_{10}$ |
| Present method               | (0)        | (1.874) | (3.419) | (3.535) | (4.641) | (4.929) | 5.104 | 5.104 | 5.699 | 5.709    |
| BEM (No. elements = 100)     | (0.308)    | (1.919) | (3.442) | (3.534) | (4.626) | (4.931) | 5.101 | 5.125 | 5.701 | 5.767    |
| ABAQUS (No. elements = 2460) | –          | –       | –       | –       | –       | –       | 5.104 | 5.104 | 5.699 | 5.709    |

Note: The data inside the parentheses denote the spurious eigenvalue, which relates to the zeros of the derivative for  $m$ th-order (even or odd) modified Mathieu functions of the first kind, ( $Je'_m(q, \xi_1)$  or  $Jo'_m(q, \xi_1)$ ).



(a) Singular formulation (UT)



(b) Hypersingular formulation (LM)

**Fig. 4.** Detection of possible eigenvalues for the free–free confocal elliptical membrane by plotting the minimum singular value  $\sigma_1$  versus  $k$  in the BEM.



**Table 5**

The former ten possible eigenvalues of a confocal elliptical membrane subject to the free–free boundary condition by using the singular BIEM/BEM and FEM.

| Method                       | Eigenvalue |       |       |       |       |       |       |         |       |          |
|------------------------------|------------|-------|-------|-------|-------|-------|-------|---------|-------|----------|
|                              | $k_1$      | $k_2$ | $k_3$ | $k_4$ | $k_5$ | $k_6$ | $k_7$ | $k_8$   | $k_9$ | $k_{10}$ |
| Present method               | 0          | 0.893 | 1.064 | 1.922 | 1.981 | 2.895 | 2.914 | (3.777) | 3.835 | 3.840    |
| BEM (No. elements = 100)     | 0          | 0.894 | 1.067 | 1.926 | 1.986 | 2.903 | 2.921 | (3.785) | 3.846 | 3.851    |
| ABAQUS (No. elements = 2460) | 0          | 0.893 | 1.064 | 1.922 | 1.981 | 2.895 | 2.913 | –       | 3.835 | 3.840    |

Note: The data inside the parentheses denote the spurious eigenvalue, which relates to the zeros of the  $m$ th-order (even or odd) modified Mathieu functions of the first kind, ( $J_m(q, \xi_1)$  or  $Jo_m(q, \xi_1)$ ).

**Table 6**

The former ten possible eigenvalues of a confocal elliptical membrane subject to the free–free boundary condition by using the hypersingular BIEM/BEM and FEM.

| Method                       | Eigenvalue |       |       |       |         |       |       |       |       |          |
|------------------------------|------------|-------|-------|-------|---------|-------|-------|-------|-------|----------|
|                              | $k_1$      | $k_2$ | $k_3$ | $k_4$ | $k_5$   | $k_6$ | $k_7$ | $k_8$ | $k_9$ | $k_{10}$ |
| Present method               | 0          | (0)   | 0.893 | 1.064 | (1.874) | 1.922 | 1.981 | 2.895 | 2.914 | (3.419)  |
| BEM (No. elements = 100)     | 0          | (0)   | 0.885 | 1.076 | (1.887) | 1.922 | 1.989 | 2.899 | 2.921 | (3.435)  |
| ABAQUS (No. elements = 2460) | 0          | –     | 0.893 | 1.064 | –       | 1.922 | 1.981 | 2.895 | 2.913 | –        |

Note: The data inside the parentheses denote the spurious eigenvalue, which relates to the zeros of the derivative for  $m$ th-order (even or odd) modified Mathieu functions of the first kind, ( $J'_m(q, \xi_1)$  or  $Jo'_m(q, \xi_1)$ ).

close to the boundary  $B$ , we obtain the following linear algebraic equations from Eqs. (10) and (11)

$$[\mathbf{U}]\{\mathbf{t}\} = [\mathbf{T}]\{\mathbf{u}\}, \quad (51)$$

$$[\mathbf{L}]\{\mathbf{t}\} = [\mathbf{M}]\{\mathbf{u}\}, \quad (52)$$

where  $[\mathbf{U}]$ ,  $[\mathbf{T}]$ ,  $[\mathbf{L}]$  and  $[\mathbf{M}]$  are influence matrices with a dimension  $N$  by  $N$ , in which  $N$  is the number of the constant element. The detailed formulation can be found in (Chen and Chen, 1998). The two column vectors of  $\{\mathbf{u}\}$  and  $\{\mathbf{t}\}$  are boundary data with a dimension of  $N$  by 1. After matching the Dirichlet or Neumann boundary conditions, we have

$$[\mathbf{U}]\{\mathbf{t}\} = \{\mathbf{0}\}, \quad (53)$$

$$[\mathbf{L}]\{\mathbf{t}\} = \{\mathbf{0}\}, \quad (54)$$

for the Dirichlet problem by using Eqs. (51) and (52), respectively, and

$$[\mathbf{T}]\{\mathbf{u}\} = \{\mathbf{0}\}, \quad (55)$$

$$[\mathbf{M}]\{\mathbf{u}\} = \{\mathbf{0}\}, \quad (56)$$

for the Neumann problem by using Eqs. (51) and (52), respectively. For the existence of non-trivial solution of  $\{\mathbf{t}\}$  or  $\{\mathbf{u}\}$ , the determinant of four influence matrices,  $[\mathbf{U}]$ ,  $[\mathbf{T}]$ ,  $[\mathbf{L}]$  and  $[\mathbf{M}]$ , at the eigenvalue of  $k$  must be zero. In other words, the minimum singular value  $\sigma_1$  of the influence matrix is equal to zero in the SVD scheme (Kuo et al., 2000; Chen et al., 2009), when  $k$  is an eigenvalue. Then, we can detect eigenvalues by plotting a figure of the minimum singular value  $\sigma_1$  versus  $k$ . The possible eigenvalues appear at the positions of drops. In the numerical implementation, we used the IMSL routine LSVCR for the SVD which is based on the LINPACK routine CSVDC (Dongarra et al., 1979).

## 5. Treatment of the spurious eigenvalues for multiply-connected eigenproblems

Regarding multiply-connected eigenproblems, the spurious eigenvalues may occur since the BEM or BIEM is employed to solve the eigenproblems. They can be seen as a combination of an interior problem and many exterior problems. The fictitious frequency of exterior problems is the source that BEM/BIEM result in spurious eigenvalues for multiply-connected eigenproblems. This is the reason why spurious eigenvalues may appear in multiply-connected eigenproblems. In order to suppress the appearance of the spurious

eigenvalues, three methods of extracting out true and spurious eigenvalues, including the CHIEF method (Chen et al., 2003), the SVD updating technique (Chen et al., 2003, 2004b, 2005, 2007, 2008b, 2009a, 2010a), and the Burton & Miller approach (Chen et al., 2001, 2007) are adopted, respectively.

### 5.1. CHIEF method

Since spurious eigenvalues result from the rank deficiency of influence matrix, we must add extra independent constrains to promote the rank of influence matrix. We employ the CHIEF method in conjunction with the SVD technique. According to the concept of CHIEF, we consider the additional collocation points in the region inside the inner boundary to obtain the null-field BIE by using Eq. (10)

$$[\mathbf{U}_{M \times N}^C]\{\mathbf{t}\} = [\mathbf{T}_{M \times N}^C]\{\mathbf{u}\}, \quad (57)$$

where the superscript  $C$  denotes collocation null-field points on the complementary domain and  $M$  is the number of CHIEF points. By combining Eq. (51) with Eq. (57), the over-determined system is obtained as

$$\begin{bmatrix} \mathbf{U}_{N \times N} \\ \mathbf{U}_{M \times N}^C \end{bmatrix} \{\mathbf{t}\} = \begin{bmatrix} \mathbf{T}_{N \times N} \\ \mathbf{T}_{M \times N}^C \end{bmatrix} \{\mathbf{u}\}. \quad (58)$$

Then, we apply the SVD technique to the assemble matrices for detecting the eigenvalues. If the CHIEF points are located on the appropriate positions, the spurious eigenvalues can be filtered out. Once the positions of CHIEF points are corresponding to the nodal lines of interior problem (Chen et al., 2003, 2009b), those points create the dependent equation and the spurious eigenvalues may still exist.

### 5.2. SVD updating technique

In this subsection, the true and spurious eigenvalues are detected by using the SVD updating terms and the SVD updating documents, respectively. These techniques have been successfully employed for rod (Chen et al., 2009a), membrane (Chen et al., 2003, 2004b, 2005, 2007), plate (Lee and Chen, 2008a,b) and concentric sphere cavity (Chen et al., 2010a). Now, we will utilize the SVD updating technique to deal with the eigenproblems containing elliptical boundaries.

### 5.2.1. SVD updating terms to extract out true eigenvalues

The true eigenvalues are dependent on the geometry and boundary conditions and independent of the formulations used. Based on the scheme of SVD updating terms, we combine Eqs. (53) and (54) as shown below:

$$\begin{bmatrix} \mathbf{U} \\ \mathbf{L} \end{bmatrix} \{\mathbf{t}\} = \{\mathbf{0}\}. \quad (59)$$

Then, the true eigenvalues of the Dirichlet boundary condition can be extracted out by plotting the minimum singular value of  $\begin{bmatrix} \mathbf{U} \\ \mathbf{L} \end{bmatrix}$  versus  $k$  free of the pollution of spurious eigenvalues. Similarly, the true eigenvalues of the Neumann boundary condition can be detected by combining Eqs. (55) and (56) as shown below:

$$\begin{bmatrix} \mathbf{T} \\ \mathbf{M} \end{bmatrix} \{\mathbf{t}\} = \{\mathbf{0}\}. \quad (60)$$

### 5.2.2. SVD updating documents to extract out spurious eigenvalues

As previously mentioned (Chen et al., 2003), spurious eigenvalues depend on the geometry of inner boundary and the approach

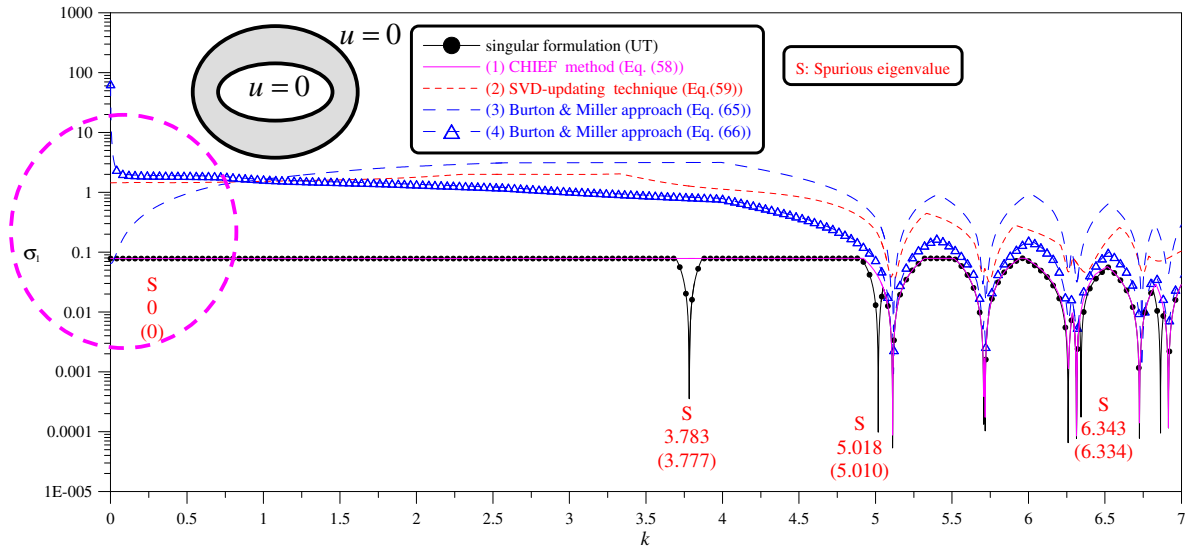
used (singular or hypersingular) instead of the types of boundary condition. When we employ the singular formulation, the spurious eigenvalues are found to be embedded in both the Dirichlet boundary condition (Eq. (53)) and Neumann boundary condition (Eq. (55)). According to the Fredholm alternative theorem, there exists a nontrivial  $\{\phi_S\}$  vector for the spurious eigenvalue  $k$

$$\begin{bmatrix} \mathbf{U}^H \\ \mathbf{T}^H \end{bmatrix} \{\phi_S\} = \{\mathbf{0}\}, \quad (61)$$

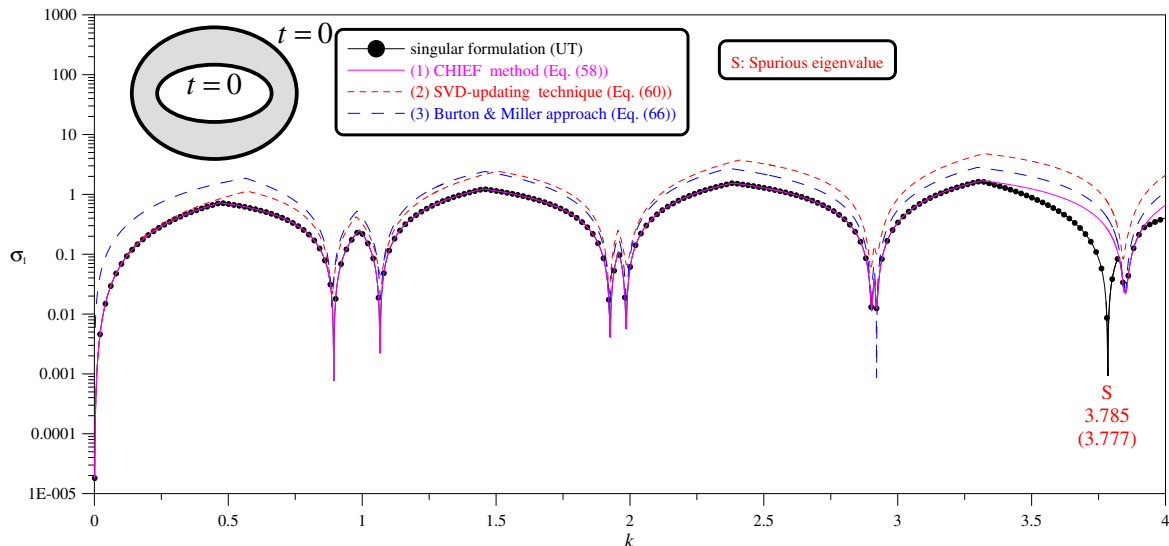
or

$$\{\phi_S\}^H [\mathbf{U} \quad \mathbf{T}] = \{\mathbf{0}\}^H, \quad (62)$$

where the superscript  $H$  denotes the Hermitian operator and  $\{\phi_S\}$  is the spurious mode corresponding to the spurious eigenvalue. The detailed derivation can be found in Chen et al. (2003). Similarly, the spurious eigenvalues of the hypersingular formulation can be detected by combining Eqs. (54) and (56) as shown below:



(a) Fixed-fixed B.C.



(b) Free-free B.C.

**Fig. 5.** Extraction of true eigenvalues for the confocal elliptical membrane by plotting the minimum singular value  $\sigma_1$  versus  $k$  through (1) CHIEF method (0.2, 0.2), (2) SVD updating technique and (3) Burton & Miller approach.

$$\begin{bmatrix} \mathbf{L}^H \\ \mathbf{M}^H \end{bmatrix} \{\bar{\phi}_S\} = \{\mathbf{0}\}, \quad (63)$$

or

$$\{\bar{\phi}_S\}^H [\mathbf{L} \ \mathbf{M}] = \{\mathbf{0}\}^H, \quad (64)$$

where  $\{\bar{\phi}_S\}$  is the spurious mode due to the hypersingular formulation.

### 5.3. Burton and Miller approach

By extending the idea of Burton & Miller approach (Chen et al., 2001, 2007) for exterior acoustics to filter out spurious eigenvalues, we combine the singular integral formulation and the hypersingular formulation with an imaginary constant in the BEM or BIEM as given below:

$$[ik[\mathbf{U}] + [\mathbf{L}]]\{\mathbf{t}\} = [ik[\mathbf{T}] + [\mathbf{M}]]\{\mathbf{u}\}. \quad (65)$$

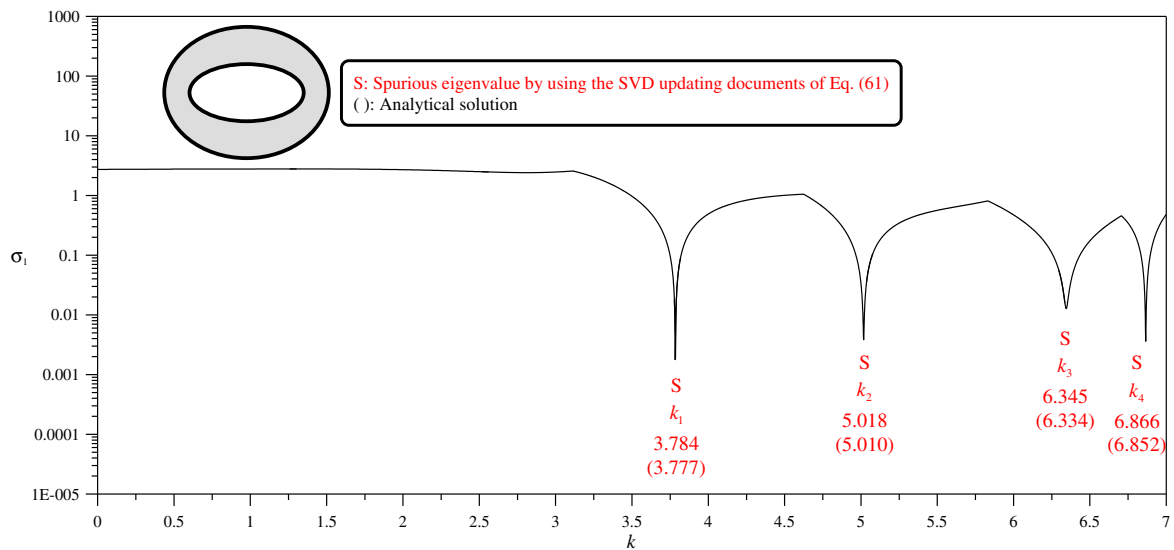
Thus, only the true eigenvalues are obtained by using the Burton & Miller approach.

## 6. Illustrative examples

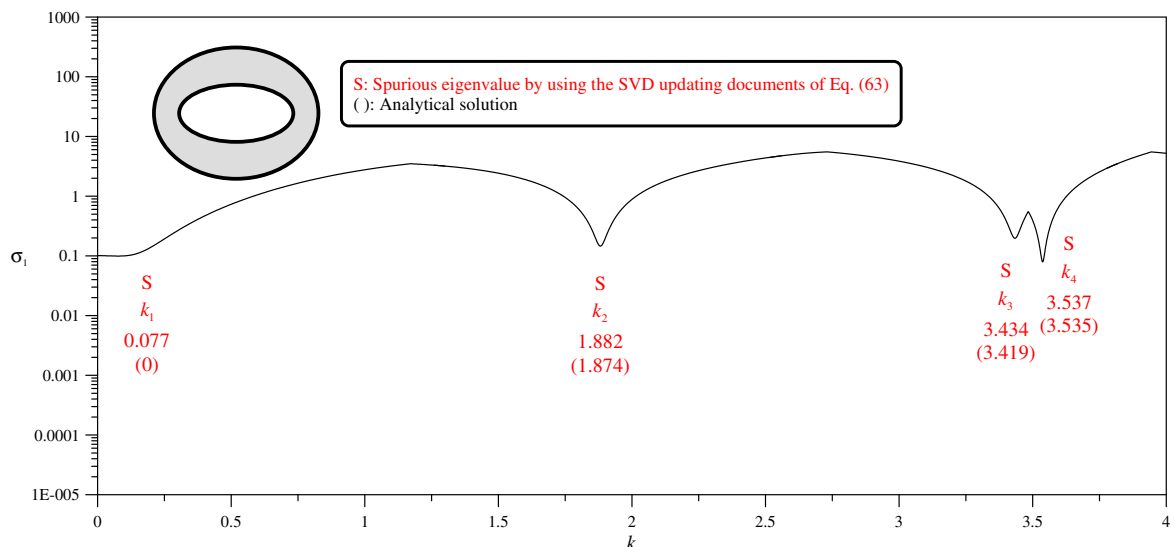
In order to demonstrate the validity of the present approaches, we consider a confocal elliptical membrane and a circular membrane containing an elliptical hole as shown in Figs. 1 and 2, respectively. The eigensolutions of the confocal case can be obtained by using the analytical derivation. Also, the FEM result is utilized for validations. Note that, the second-order acoustic elements AC2D8 of ABAQUS are adopted in the mesh of the finite-element models.

### 6.1. A confocal elliptical membrane

In this case, a confocal elliptical membrane is considered. The half lengths of major and minor for the inner boundary are  $a_1 = 1$  and  $b_1 = 0.5$ , respectively. The radial parameter  $\xi$  of the inner boundary is  $\xi_1 = \tanh^{-1}(b_1/a_1)$  and the outer boundary is described by  $\xi_0 = 2\xi_1$ . Figs. 3(a) and (b) show the minimum singular value versus  $k$  for the fixed-fixed boundary condition. Note that, the drops indicate the possible eigenvalues by using the singular for-



(a) Singular formulation (UT)



(b) Hypersingular formulation (LM)

Fig. 6. Extraction of spurious eigenvalues in the BEM by plotting the minimum singular value  $\sigma_1$  versus  $k$  in the SVD updating documents.

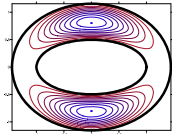
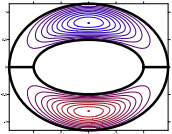
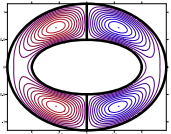
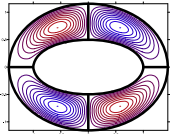
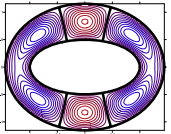
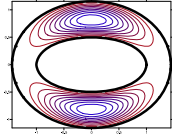
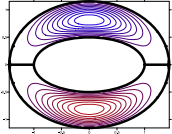
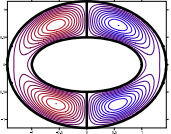
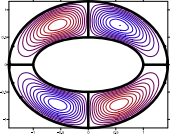
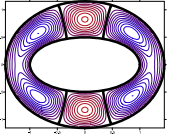
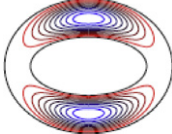
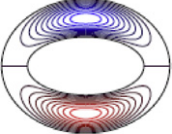
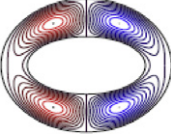
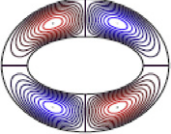
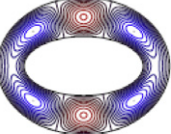
mulation (Eq. (53)) and hypersingular formulation (Eq. (54)), respectively. To summarize, we list the former ten possible eigenvalues in Tables 3 and 4 including the results of the analytical solutions and the FEM. Good agreement is made. It is found that no spurious eigenvalues appear in the data of FEM. True and spurious eigenvalues are analytically predicted and numerically verified by using the BIEM and BEM, respectively. The true eigenvalue of  $k = 5.112$  has algebraic multiplicity two since the rank deficiency of the  $[\mathbf{U}]$  is equal to two. Furthermore, the eigenvalue of  $k = 5.104$  can be analytically predicted from Eq. (45) ( $m = 0$ ) and (46) ( $m = 1$ ). For the free-free boundary condition, Figs. 4(a) and (b) show the minimum singular value versus  $k$  by using the singular formulation (Eq. (55)) and hypersingular formulation (Eq. (56)), respectively. The former ten possible eigenvalues are listed in Tables 5 and 6. It is interesting that the zero eigenvalue is not only

the true eigenvalue but also the spurious eigenvalue. To suppress the spurious eigenvalues, the CHIEF method, the SVD updating technique and the Burton & Miller approach are used, respectively. Fig. 5(a) show the minimum singular value versus  $k$  for the fixed-fixed boundary condition by using the three approaches. Spurious eigenvalues do not appear in Fig. 5(a), but it is amazing that the zero spurious eigenvalue still exists. Nevertheless, it is reasonable since the zero eigenvalue is simultaneously imbedded in the  $ik[\mathbf{U}]$  and  $[\mathbf{L}]$  matrices. In order to suppress the zero spurious eigenvalue, we modify the combination of Burton & Miller approach in Eq. (65) as shown below:

$$[\mathbf{U}] - \frac{i}{k}[\mathbf{L}]\{\mathbf{t}\} = [\mathbf{T}] - \frac{i}{k}[\mathbf{M}]\{\mathbf{u}\}. \quad (66)$$

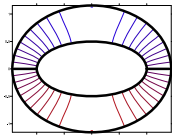
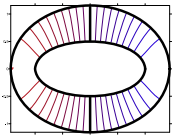
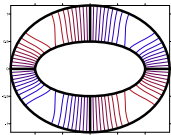
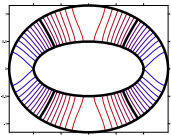
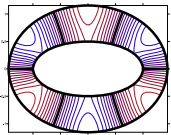
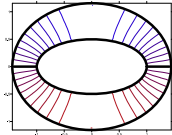
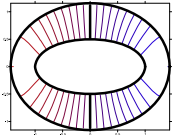
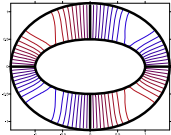
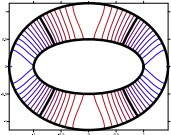
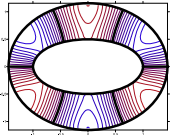
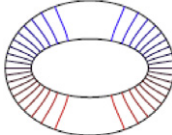
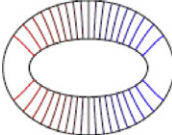
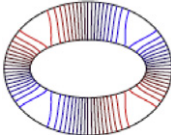
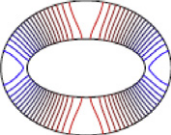
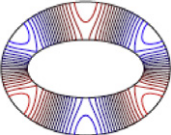
**Table 7**

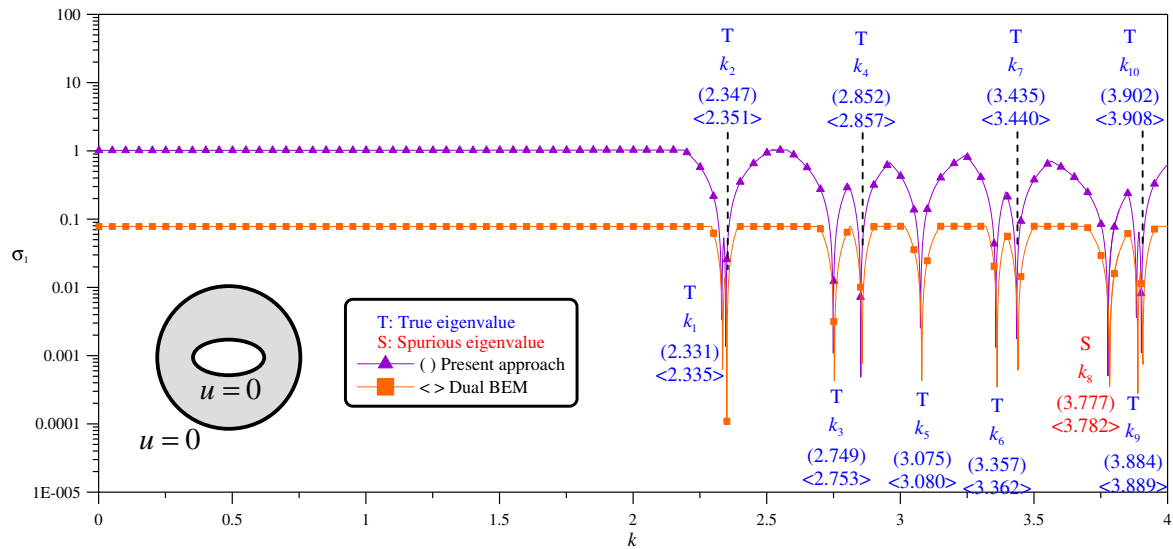
The former five modes for a confocal elliptical membrane subject to the fixed-fixed boundary condition.

| Method                        | Eigenmode   |   |  |   |   |
|-------------------------------|---|---|--|---|---|
|                               | Mode 1  | Mode 2  | Mode 3   | Mode 4  | Mode 5  |
| Present method                |    |    |    |    |    |
|                               | $k = 5.104$   | $k = 5.104$   | $k = 5.699$  | $k = 5.709$   | $k = 6.251$   |
| BEM (UT) (No. elements = 100) |   |   |   |   |   |
|                               | $k = 5.112$   | $k = 5.112$   | $k = 5.707$  | $k = 5.717$   | $k = 6.259$   |
| ABAQUS (No. elements = 2460)  |  |  |  |  |  |
|                               | $k = 5.104$   | $k = 5.104$   | $k = 5.699$  | $k = 5.709$   | $k = 6.251$   |

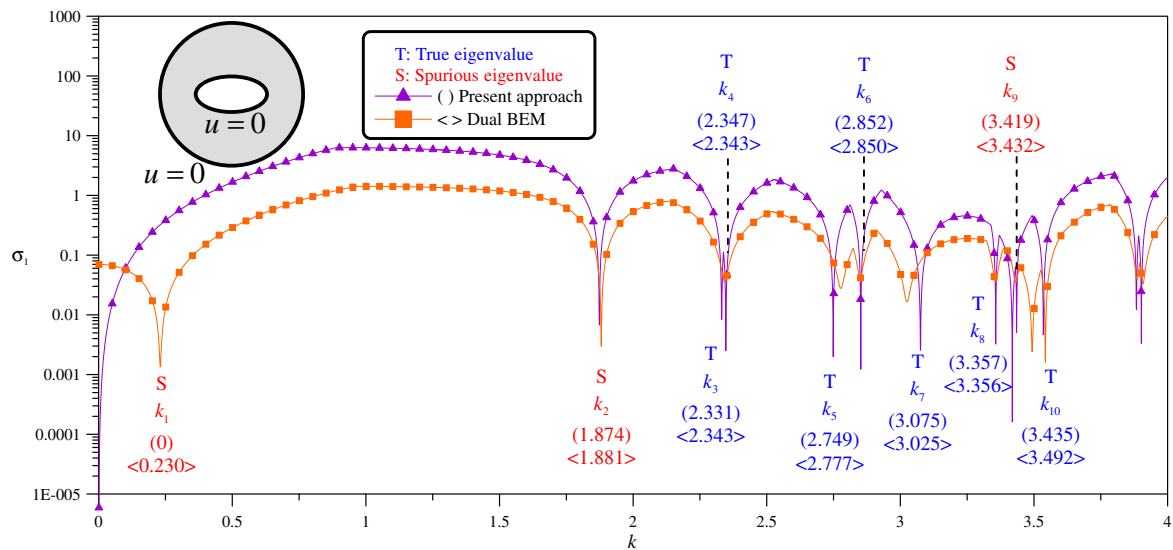
**Table 8**

The former six modes (not including the first rigid body mode) for a confocal elliptical membrane subject to the free-free boundary condition.

| Method                        | Eigenmode   |   |  |   |   |
|-------------------------------|---|---|--|---|---|
|                               | Mode 2  | Mode 3  | Mode 4   | Mode 5  | Mode 6  |
| Present method                |  |  |  |  |  |
|                               | $k = 0.893$   | $k = 1.064$   | $k = 1.922$  | $k = 1.981$   | $k = 2.895$   |
| BEM (UT) (No. elements = 100) |  |  |  |  |  |
|                               | $k = 0.894$   | $k = 1.067$   | $k = 1.926$  | $k = 1.986$   | $k = 2.903$   |
| ABAQUS (No. elements = 2460)  |  |  |  |  |  |
|                               | $k = 0.893$   | $k = 1.064$   | $k = 1.922$  | $k = 1.981$   | $k = 2.895$   |



(a) Singular formulation (UT)



(b) Hypersingular formulation (LM)

**Fig. 7.** Detection of possible eigenvalues for the case 2 by plotting the minimum singular value  $\sigma_1$  versus  $k$  in the BIEM and BEM.**Table 9**

The former ten possible eigenvalues of a confocal elliptical membrane subject to the free–free boundary condition by using the singular BIEM/BEM and FEM.

| Method                          | Eigenvalue |       |       |       |       |       |       |         |       |          |
|---------------------------------|------------|-------|-------|-------|-------|-------|-------|---------|-------|----------|
|                                 | $k_1$      | $k_2$ | $k_3$ | $k_4$ | $k_5$ | $k_6$ | $k_7$ | $k_8$   | $k_9$ | $k_{10}$ |
| Present method (No. nodes = 42) | 2.331      | 2.347 | 2.749 | 2.852 | 3.075 | 3.357 | 3.435 | (3.777) | 3.884 | 3.902    |
| BEM (No. elements = 100)        | 2.335      | 2.351 | 2.753 | 2.857 | 3.080 | 3.362 | 3.440 | (3.782) | 3.889 | 3.908    |
| ABAQUS (No. elements = 2460)    | 2.331      | 2.347 | 2.749 | 2.852 | 3.075 | 3.357 | 3.435 | –       | 3.884 | 3.902    |

Note: The data inside the parentheses denote the spurious eigenvalue, which relates to the zeros of the  $m$ th-order (even or odd) modified Mathieu functions of the first kind,  $(J_m(q, \xi_1))$  or  $(J'_m(q, \xi_1))$ .

**Table 10**

The former ten possible eigenvalues of a confocal elliptical membrane subject to the free–free boundary condition by using the hypersingular BIEM/BEM and FEM.

| Method                          | Eigenvalue |         |       |       |       |       |       |       |         |          |
|---------------------------------|------------|---------|-------|-------|-------|-------|-------|-------|---------|----------|
|                                 | $k_1$      | $k_2$   | $k_3$ | $k_4$ | $k_5$ | $k_6$ | $k_7$ | $k_8$ | $k_9$   | $k_{10}$ |
| Present method (No. nodes = 42) | (0)        | (1.874) | 2.331 | 2.347 | 2.749 | 2.852 | 3.075 | 3.357 | (3.419) | 3.435    |
| BEM (No. elements = 100)        | (0.230)    | (1.881) | 2.343 | 2.343 | 2.777 | 2.850 | 3.025 | 3.356 | (3.432) | 3.492    |
| ABAQUS (No. elements = 2460)    | –          | –       | 2.331 | 2.347 | 2.749 | 2.852 | 3.075 | 3.357 | –       | 3.435    |

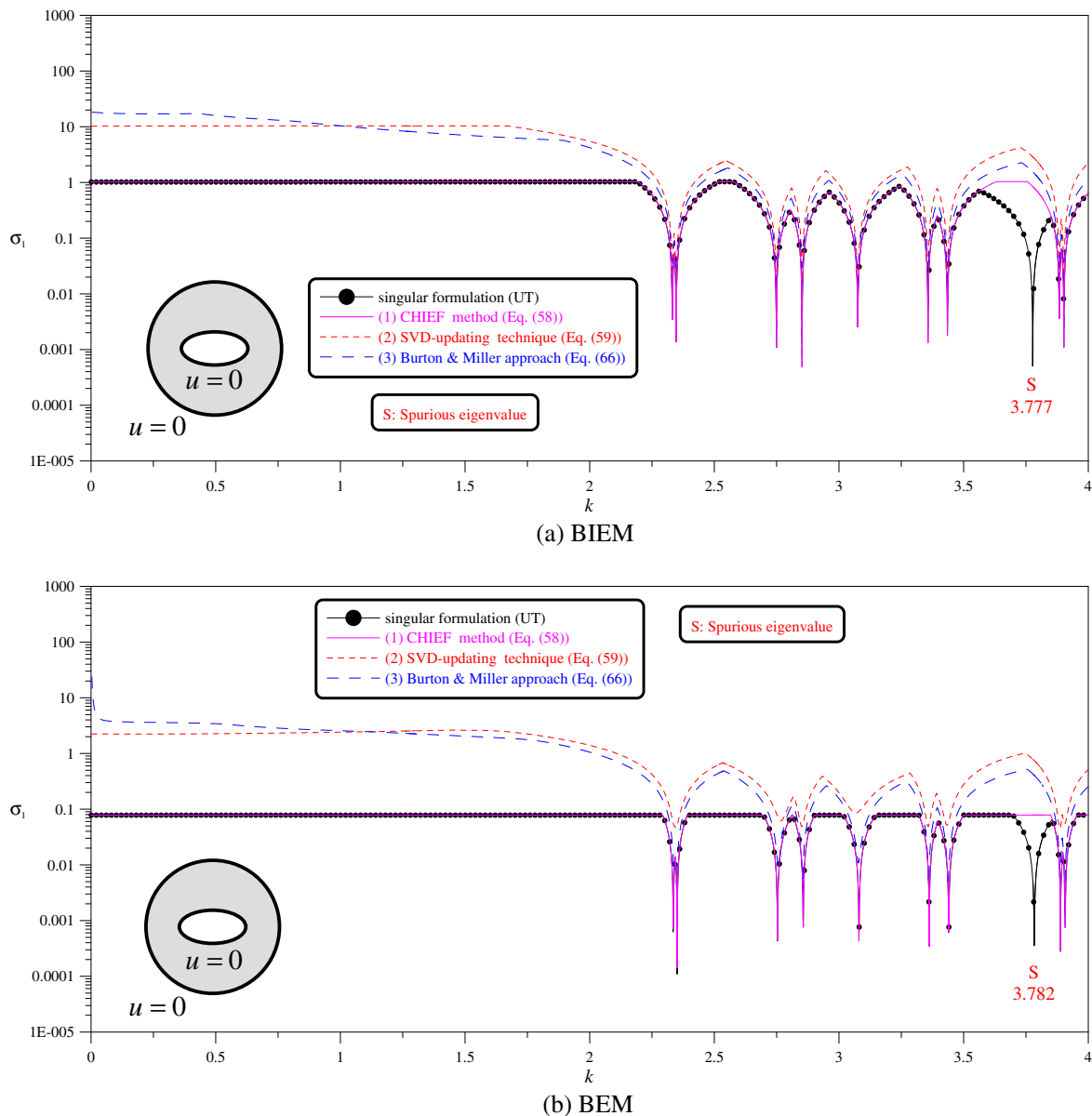
Note: The data inside the parentheses denote the spurious eigenvalue, which relates to the zeros of the derivative for  $m$ th-order (even or odd) modified Mathieu functions of the first kind,  $(J'_m(q, \xi_1))$  or  $(J_m(q, \xi_1))$ .



Then, the result is shown in Fig. 5(a) and spurious eigenvalue of zero is not found. In the same way, the plot of minimum singular value versus  $k$  for the free–free boundary condition is shown in Fig. 5(b). Besides, the spurious eigenvalues can be extracted out by using the SVD updating documents technique as shown in Fig. 6. Although true eigenvalues can be detected by using the CHIEF method and the Burton & Miller approach, respectively, spurious eigenvalues cannot. Nevertheless, true and spurious eigenvalues can be extracted out by using the SVD updating terms and documents, respectively. Tables 7 and 8 show the former five eigenmodes of the fixed–fixed and free–free boundary conditions, respectively. The first mode is symmetric with respect to the  $x$ -axis, while the second mode is antisymmetric with respect to the  $x$ -axis. The eigenvalue of the symmetric mode is corresponding to the zeros of true eigenequation Eq. (45). On the contrary, the eigenvalue of the antisymmetric mode is corresponding to the zeros of Eq. (46).

## 6.2. A circular membrane containing an elliptical hole

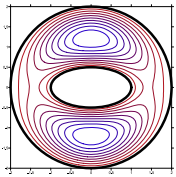
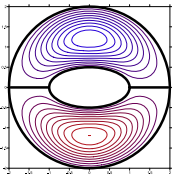
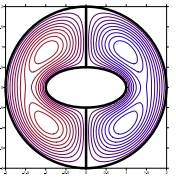
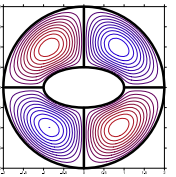
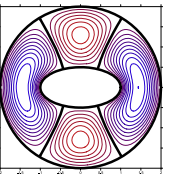
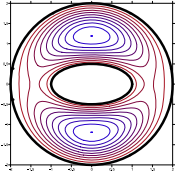
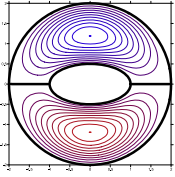
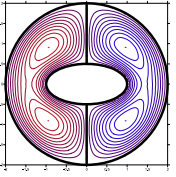
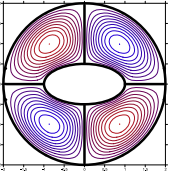
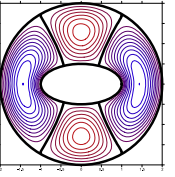
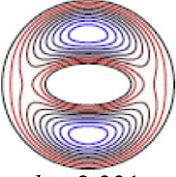
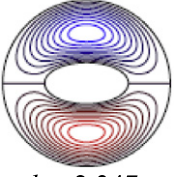
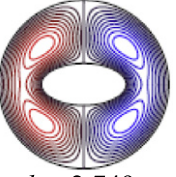
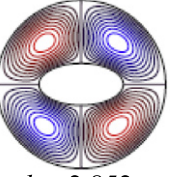
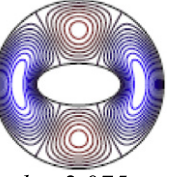
In the second case, a circular membrane containing an elliptical hole is considered. The radius of the outer boundary is  $r_0 = 2$  while the geometric parameter of inner elliptical boundary is the same with that of the confocal elliptical membrane of case 1. The fixed–fixed boundary condition is considered. Based on the adaptive observer system and vector decomposition technique [21], this problem can be solved without any difficulty by using the BIEM. Figs. 7(a) and (b) show the minimum singular value versus  $k$  by using the singular formulation and hypersingular formulation, respectively. The former ten possible eigenvalues are listed in Tables 9 and 10 and are compared with those of the FEM. Good agreement is made. It is interesting that the spurious eigenvalues are equal to those of the confocal case since the inner boundary is the same. These results support the finding that the spurious eigenvalues depend on the geometry of inner boundary and the



**Fig. 8.** Extraction of true eigenvalues for the case 2 by plotting the minimum singular value  $\sigma_1$  versus  $k$  through (1) CHIEF method (0.2, 0.2), (2) SVD updating technique and (3) Burton & Miller approach.

**Table 11**

The former five modes for a circular membrane containing an elliptical hole subject to the fixed–fixed boundary condition.

| Method                          | Eigenmode  |  |   |  |  |
|---------------------------------|--|--|---|--|--|
|                                 | Mode 1   | Mode 2   | Mode 3  | Mode 4   | Mode 5   |
| Present method (No. nodes = 42) | <br>$k = 2.331$ | <br>$k = 2.347$ | <br>$k = 2.749$ | <br>$k = 2.852$ | <br>$k = 3.075$ |
| BEM (UT) (No. elements = 100)   | <br>$k = 2.335$ | <br>$k = 2.351$ | <br>$k = 2.753$ | <br>$k = 2.857$ | <br>$k = 3.080$ |
| ABAQUS (No. elements = 2460)    | <br>$k = 2.331$ | <br>$k = 2.347$ | <br>$k = 2.749$ | <br>$k = 2.852$ | <br>$k = 3.075$ |

approach used once again. We also employ three methods to extract out the true eigenvalues as shown in Fig. 8. In addition, the former five eigenmodes are shown in Table 11.

## 7. Conclusions

In this paper, analytical derivation of the true and spurious eigenvalues for confocal elliptical membrane has been made successfully by applying the BIEM in conjunction with the separable kernels and eigenfunction expansion. Numerical results using the BEM and FEM also acquired, respectively, and match well with those predicted theoretically in terms of the true and spurious eigenvalues.

By the analytical derivation, it is revealed that spurious eigenvalues depend on the geometry of inner boundary and the approach used. This finding is the same with those corresponding to the annular cases. Also, the finding is further confirmed numerically through illustrative examples of a confocal elliptical membrane and a circular membrane containing an elliptical hole.

Besides, we employed the CHIEF method, the SVD updating technique and the Burton & Miller approach to suppress the appearance of spurious eigenvalues for the multiply-connected problems. It is found that the CHIEF method is more efficient than the SVD updating technique and the Burton & Miller approach due to no hypersingularities involved and less computational effort.

## Acknowledgement

Financial support from the National Science Council under Grant No. NSC-98-2221-E-019-017-MY3 for National Taiwan Ocean University is gratefully acknowledged.

## References

Abramowitz, M., Stegun, I.A., 1965. Handbook of Mathematical Functions with Formulas, Graphs and Mathematical Tables. Dover, New York.

- Burton, A.J., Miller, G.F., 1971. The application of integral equation methods to numerical solution of some exterior boundary value problems. *Proc. Roy. Soc. Lond. A* 323, 201–210.
- Chen, J.T., Chen, K.H., 1998. Dual integral formulation for determining the acoustic modes of a two-dimensional cavity with a degenerate boundary. *Eng. Anal. Bound. Elem.* 21 (2), 105–116.
- Chen, J.T., Lin, J.H., Kuo, S.R., Chyuan, S.W., 2001. Boundary element analysis for the Helmholtz eigenvalue problems with a multiply-connected domain. *Proc. Roy. Soc. Lond. A* 457, 2521–2546.
- Chen, J.T., Chang, M.H., Chung, I.L., Cheng, Y.C., 2002. Comment on “Eigenmode analysis of arbitrarily shaped two-dimensional cavities by the method of point matching”. *J. Acoust. Soc. Am.* 111 (1 Part 1).
- Chen, J.T., Liu, L.W., Hong, H.-K., 2003. Spurious and true eigensolutions of Helmholtz BIEs and BEMs for a multiply-connected problem. *Proc. Roy. Soc. Lond. A* 459, 1891–1925.
- Chen, J.T., Lin, S.Y., Chen, K.H., Chen, I.L., 2004a. Mathematical analysis and numerical study of true and spurious eigenequations for free vibration of plates using real-part BEM. *Comput. Mech.* 34, 165–180.
- Chen, J.T., Liu, L.W., Chyuan, S.W., 2004b. Acoustic eigenanalysis for multiply-connected problems using dual BEM. *Commun. Numer. Meth. Eng.* 20, 419–440.
- Chen, J.T., Chen, I.L., Lee, Y.T., 2005. Eigensolutions of multiply connected membranes using the method of fundamental solutions. *Eng. Anal. Bound. Elem.* 29, 166–174.
- Chen, J.T., Chen, C.T., Chen, I.L., 2007. Null-field integral equation approach for eigenproblems with circular boundaries. *J. Comput. Acoust.* 15 (4), 401–428.
- Chen, J.T., Lee, J.W., Cheng, Y.C., 2009a. On the spurious eigensolutions for the real-part boundary element method. *Eng. Anal. Bound. Elem.* 33, 342–355.
- Chen, J.T., Lin, S.R., Tsai, J.J., 2009b. Fictitious frequency revisited. *Eng. Anal. Bound. Elem.* 33, 1289–1301.
- Chen, J.T., Kao, S.K., Lee, Y.T., Lin, Y.J., 2010a. On the spurious eigenvalues for a concentric sphere in BIEM. *Appl. Acoust.* 71, 181–190.
- Chen, J.T., Lee, Y.T., Lee, J.W., 2010b. Torsional rigidity of an elliptic bar with multiple elliptic inclusions using the null-field integral approach. *Comput. Mech.* 46, 511–519.
- Courant, R., Hilbert, D., 1989. *Methods of Mathematical Physics*. John Wiley & Sons, New York.
- De Mey, G., 1976. Calculation of eigenvalues of the Helmholtz equation by an integral equation. *Int. J. Numer. Meth. Eng.* 10, 59–66.
- De Mey, G., 1977. A simplified integral equation method for the calculation of the eigenvalues of Helmholtz equation. *Int. J. Numer. Meth. Eng.* 11, 1340–1342.
- Dongarra, J.J., Bunch, J.R., Moler, C.B., Stewart, G.W., 1979. *LINPACK Users' Guide*. SIAM, Philadelphia.
- Duran, M., Miguez, M., Nedelec, J.C., 2001. Numerical stability in the calculation of eigenfrequencies using integral equations. *J. Comput. Appl. Math.* 130, 323–336.
- Hong, K., Kim, J., 1995. Natural mode analysis of hollow and annular elliptical cylindrical cavities. *J. Sound Vib.* 183 (2), 327–351.

- Hutchinson, J.R., Wong, G.K.K., 1979. The boundary element method for plate vibrations. In: *Proceedings of the ASCE Seventh International Conference on Electronic Computation*, pp. 297–311.
- Hutchinson, J.R., 1984. Boundary method for time-dependent problems. In: *Proceedings of the Fifth Engineering Mechanics Division Conference*. ASCE, WY, pp. 136–139.
- Kamiya, N., Andoh, E., Nogae, K., 1996. A new complex-valued formulation and eigenvalue analysis of the Helmholtz equation by boundary element method. *Adv. Eng. Softw.* 26, 219–227.
- Kang, S.W., Lee, J.M., Kang, Y.J., 1999. Vibration analysis of arbitrarily shaped membranes using non-dimensional dynamic influence function. *J. Sound Vib.* 234 (1), 455–470.
- Kitahara, M., 1985. *Boundary Integral Equation Methods in Eigenvalue Problems of Elastodynamics and Thin Plates*. Elsevier Science, Amsterdam.
- Kobayashi, S., Nishimura, N., 1982. Developments in boundary element methods-2. In: Banerjee, P.K., Shaw, R.P. (Eds.). *Applied Science Publishers*, pp. 177–210.
- Kuo, S.R., Chen, J.T., Huang, C.X., 2000. Analytical study and numerical experiments for true and spurious eigensolutions of a circular cavity using the real-part dual BEM. *Int. J. Numer. Meth. Eng.* 48, 1401–1422.
- Lee, W.M., Chen, J.T., 2008a. Analytical study and numerical experiments of true and spurious eigensolutions of free vibration of circular plates using real-part BEM. *Eng. Anal. Bound. Elem.* 32, 368–387.
- Lee, W.M., Chen, J.T., 2008b. Null-field integral equation approach for free vibration analysis of circular plates with multiple circular holes. *Comput. Mech.* 42, 733–747.
- Morse, P., Feshbach, H., 1953. *Method of Theoretical Physics*. McGraw-Hill, New York.
- Schenck, H.A., 1968. Improved integral formulation for acoustic radiation problem. *J. Acoust. Soc. Am.* 44, 41–58.
- Seybert, A.F., Rengarajan, T.K., 1987. The use of CHIEF to obtain unique solutions for acoustic radiation using boundary integral equations. *J. Acoust. Soc. Am.* 81, 1299–1306.
- Tai, G.R.G., Shaw, R.P., 1974. Helmholtz equation eigenvalues and eigenmodes for arbitrary domains. *J. Acoust. Soc. Am.* 56, 796–804.
- Troesch, B.A., Troesch, H.R., 1973. Eigenfrequencies of an elliptic membrane. *Math. Comp.* 27 (124), 755–765.
- Yasko, M., 2000. BEM with the real-valued fundamental solutions for the Helmholtz equation. In: *Proceedings of the Seventh International Congress of Sound and Vibration*. Germany, pp. 2037–2044.
- Yeih, W., Chen, J.T., Chen, K.H., Wong, F.C., 1998. A study on the multiple reciprocity method and complex-valued formulation for the Helmholtz equation. *Adv. Eng. Softw.* 29 (1), 1–6.
- Zhang, S., Jin, J., 1996. *Computation of Special Functions*. John Wiley & Sons, New York.